IMPROVEMENT IN THE PERFORMANCE OF 3G WIRELESS COMMUNICATIONS SYSTEMS USING AN ICA BASED SIGNAL PROCESSING BLOCK

by

WINSTON DSOUZA

Presented to the Faculty of the Graduate School of

The University of Texas at Arlington in Partial Fulfillment

of the Requirements

for the Degree of

MASTER OF SCIENCE IN ELECTRICAL ENGINEERING

THE UNIVERSITY OF TEXAS AT ARLINGTON

AUGUST 2011

ACKNOWLEDGEMENTS

I would like to sincerely thank my guide and mentor, Dr. Venkat Devarajan for his support, time and advice throughout my thesis work. This thesis would not have been possible without his expert guidance and innovative ideas.

I would like to acknowledge Dr. Michael Manry and Dr. R. Stephen Gibbs for being a part of my committee. I would also like to thank all the professors from University of Texas at Arlington as well as University of Mumbai, who taught me several courses, which helped me understand the basic concepts needed for my research work. I am grateful to all my lab mates, friends and colleagues for their constant encouragement and motivation. I would also like to extend my thanks to the University of Texas at Arlington for providing me the computing and library resources, which helped towards the completion of the thesis.

Last but not least, I would like to thank my parents for their unconditional support, both emotional and financial throughout my degree. I would like to thank my sister for giving me constant encouragement and inspiration to complete my degree.

July 14, 2011

ABSTRACT

IMPROVEMENT IN THE PERFORMANCE OF 3G WIRELESS COMMUNICATIONS

SYSTEMS USING AN ICA BASED

SIGNAL PROCESSING

BLOCK

Winston Dsouza, M.S.

The University of Texas at Arlington, 2011

Supervising Professor: Venkat Devarajan

In this thesis, we have implemented a signal processing block in the receiver of a third generation (3G) cellular system to provide improvement in the quality of service. Each block of the cellular system, including the complete transmitter, channel and the receiver is implemented in Matlab. The multiplexing scheme is implemented using wideband code division multiple access (WCDMA). The signal processing block is based on the concept of independent component analysis (ICA), and a rake receiver is used at the receiver to mitigate inter symbol interference due to the multi-paths. The signal processing block (SPB) is further extended to a High Speed Downlink Packet Access System (HSDPA), whose downlink physical layer is implemented in Matlab.

The simulation is run in Matlab for a thousand frames containing different information bits, and under different channel conditions to prove that the system works for all possible case in accordance with a Monte Carlo simulation. Performance analysis is accomplished by calculating the bit error rate between the transmitted and received data. Two different calculations are performed, one with the signal processing block in place and the other without,

and a comparison is made using a SNR (signal to noise ratio) vs. BER (bit error rate) plot. Further, to extend the importance of the system to data applications, frame error rate calculation is also carried out, and a similar comparison made.

Finally, we have been able to conclude, that the performance of the 3G wireless system with the signal processing block is better than the one without it. This confirms the earlier results which were proved for second generation systems. [1, 2]

TABLE OF CONTENTS

LIST OF ILLUSTRATIONS

LIST OF TABLES

CHAPTER 1

INTRODUCTION

1.1 Background

There has been tremendous growth in telecommunications industry, since the invention of telephone by Alexander Graham Bell in 1870. Today, the global consumer base for cellular phones is more than four billion. With such a high demand for wireless communications, it is necessary to make continuous improvements to the existing systems, in order to provide good quality services to the end users as well as compete with the existing wire line services.

The first generation cellular systems were analog systems, such as AMPS (Advanced Mobile Phone systems) introduced in the United States in the 1980's. These systems were succeeded by second generation (2G) digital systems, such as Global System for Mobile (GSM) communications, US-TDMA (IS-136), cdmaOne (IS-95). Second generation systems were basically designed for voice traffic, and did not provide the required throughput for data. This led to an evolution in 2G technologies, leading to the implementation of enhanced data rate for GSM evolution (EDGE) to provide data communication, along with the voice traffic. However, it failed to provide the data rate required for applications such as fast internet browsing, video buffering etc. This led to further development of new radio interface technologies together known as third generation (3G) systems [5].

However, even with these advanced technologies in place, call drops are still existent in the system today. A call drop is defined as the unexpected termination of the voice call. It happens when the bit error rate of the signal reaching the user handset exceeds a pre-defined threshold. Due to this high BER, the User Equipment is unable to provide the required voice quality required by the network, and hence, the call is terminated.

Call drops occur due to a variety of reasons [1, 2]:

- Handover (Handoff) failure
- Network congestion
- High Bit Error rate
- Co-channel and adjacent channel interference
- Lack of coverage in a particular area

The various approaches to reduce call drops due to network congestion include dynamic channel assignment, handoff prioritization, and call admission control. While call drops due to high BER can be reduced by diversity implementation, channel coding and channel equalizer [1, 2]. Even with all these methods in place, there are still call drops. The results of a call drop survey conducted by ChangeWave Research in March of 2011 are shown in figure 1.1. The customers were asked to provide the average percentage of call drops in the past ninety days. We can see from the graph that, there is still significant amount of call drops present in the wireless systems provided by different cellular companies.

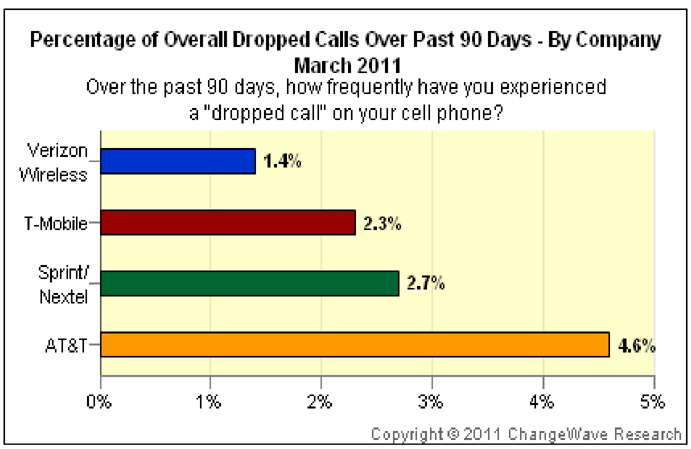

Figure 1.1 Percentage Call Drops according to customer survey taken in March 2011.

In order to understand why calls drop, we need to get an understanding of the handover process. A handover takes place when the user moves from one cell to another, when a call is in progress. A soft handover takes place, when the user moves through cells belonging to different Node B's (base stations), while softer handover takes place, when the user moves between two sectors belonging to the same Node B. In both cases, the two separately received signals are combined together using rake reception at the user terminal in the downlink direction. One of the conditions for the successful combination is that the two frames should be received successfully, by the user terminal with low BER within 50ms of each other [6].

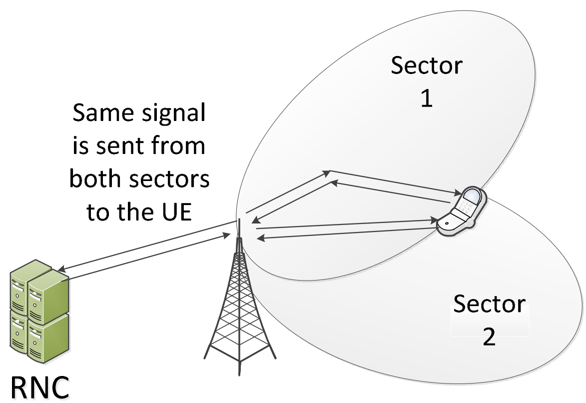

a)

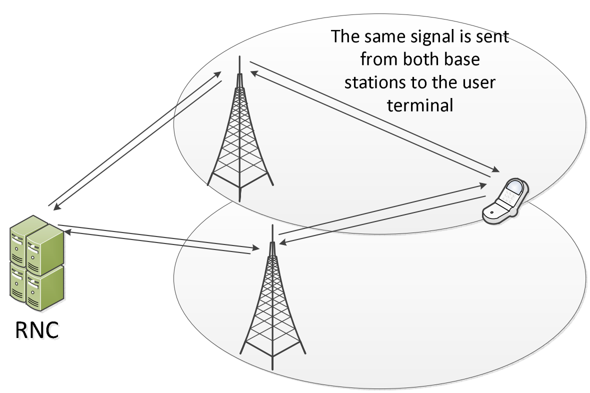

b)

Figure 1.2 Types of Handover a) Softer b) Soft [6].

Other possible handovers include inter-frequency hard handovers, where the user channel is shifted from one WCDMA frequency carrier to another, and inter-system hard handovers, where the user shifts from a WCDMA system to some other system such as GSM [6]. Both hard handovers are similar to those taking place in GSM systems, where the received signal from both base stations is continuously measured at the handset, and the handover takes place, when the received signal strength from the current base station drops below a pre-defined threshold.

A call drop can occur, when a successful handover does not take place due to very high BER. The received signal at the user terminal is corrupted by noise, which is responsible for the high BER. The basic motivation behind our development of the signal processing block was to reduce this high BER by the separation of the signal and the noise at the receiver using independent component analysis, and thus decrease the number of call drops due to handover failure.

1.2 Overview

The main objective of this thesis is to verify that the Signal Processing Block (SPB) works for an existing 3G cellular system, and prove that its introduction improves the overall performance of the system. To this effect, a complete simulation of the physical layer of a third generation frequency division duplex (FDD) system was carried out, and the BER measured for a set of thousand different frames.

The thesis is organized as follows; independent component analysis is described in detail in chapter two. The third generation systems are explained in chapter three. Chapter four and five are used to describe the transmitter section of the physical layer, and chapter six is used to give an explanation about the channel and the noise model. The receiver section is explained in chapter seven, and chapter nine is used to explain the application of SPB for a

High Speed Downlink Packet Access System (HSDPA) system. The results of the performance analysis of both the systems using SPB are explained in chapter nine.

CHAPTER 2

SIGNAL PROCESSING BLOCK

2.1 Introduction to Independent Component Analysis

Independent Component Analysis belongs to a class of blind source separation (BSS) methods, for separating data into underlying informational components, where such data can take the form of images, sounds, telecommunication channels or stock market prices. [3]. ICA takes advantage of the statistical independence between the source signals. The applications of ICA include analyzing electroencephalogram (EEG) signals, feature extraction for image, audio, video, and making predictions with regards to stock market.

For example, consider a room with two microphones, and two voice sources as shown in figure 2.1. If both the voice sources are transmitting simultaneously, then at each of the microphones we will receive a weighted mixture of the two signals.

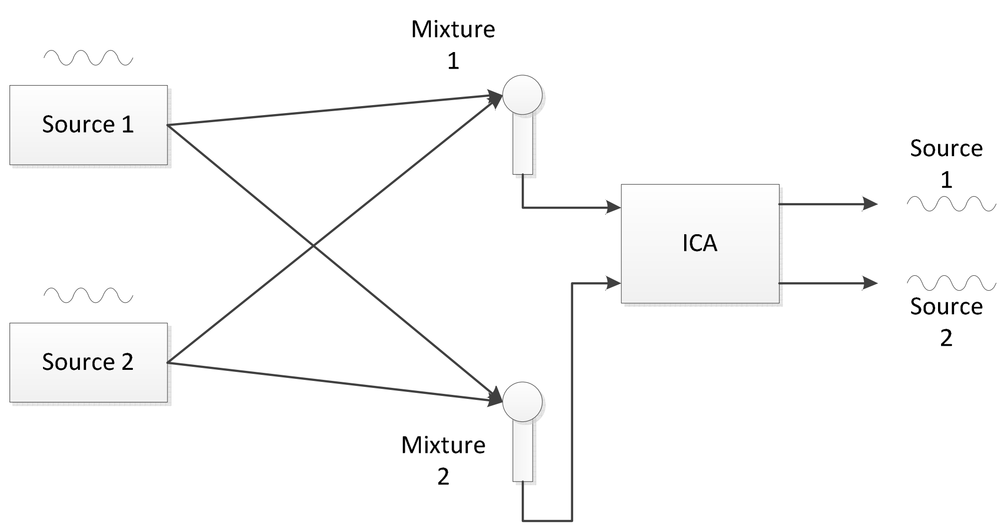

Figure 2.1 Classical Problem solved by ICA [1, 2].

The two mixtures at the microphones can be represented as

$$x_1(t) = a_{11}s_1(t) + a_{12}s_2(t)$$

$$x_2(t) = a_{21}s_1(t) + a_{22}s_2(t)$$

where $s_1(t)$ and $s_2(t)$ represent the two voice sources.

In matrix form, the above two equations can be written as

$$\begin{bmatrix} x_1 \\ x_2 \end{bmatrix} = \begin{bmatrix} a_{11} & a_{12} \\ a_{21} & a_{22} \end{bmatrix} \begin{bmatrix} s_1 \\ s_2 \end{bmatrix}$$

$$X = AS$$

Since, each of the signals $s_1(t)$ and $s_2(t)$ are from two different independent sources, at any given time *'t'*, the signal amplitudes would also be independent of each other. This property of statistical independence is used by ICA to recover the original two source signals from the two mixtures available at the microphones.

In general, we can define a matrix $W = A^{-1}$, such that

$$S = A^{-1}X = WX$$

Where W is known as the un-mixing matrix and can be calculated by using information-maximization principle in ICA [1].

2.2 Signal Processing Block

In wireless communication systems, the transmitted signal arriving at the receiver is corrupted by AWGN (Additive White Gaussian Noise). Our basic aim is to reduce the noise component of the signal, using the signal processing block at the receiver. One important requirement in ICA is that, there must be at least as many different signal mixtures available, as the number of source signals. But for our example, we have a single mixture with two sources - signal and noise. To solve this problem, we develop a second mixture by adding noise to the available mixture at the receiver. The added noise is also AWGN and is generated from a similar noise model [2].

2.3 Initial Implementation of Signal Processing Block

The received signal at the mobile terminal is corrupted by noise. The flowchart shown in figure 2.1 was first developed, and implemented to reduce the noise at the receiver. The idea for the flowchart was provided by Dr. Devarajan, and its implementation carried out collectively by Sudeep Sharma and Kumarabhijeet Singh [1, 2].

The algorithm consists of first defining a threshold such that, any voice signal, which is above this threshold is said to have good quality. This signal is stored, and its pitch is calculated by using the HPS (Harmonic Product Spectrum) algorithm [4]. If the received signal quality falls below the threshold, then the noisy signal is fed to the ICA block. The ICA block separates the noise and the voice signal from the mixture. In order to detect the voice signal, the pitch of both the output signals from the ICA block is computed, and compared with the pitch of the stored good quality signal. The pitch of the extracted voice signal will be similar to the pitch of the stored sample, while that of the noise will be random. After the above process, we obtain a reasonably noise free voice signal [1].

2.4 Application of ICA to digital signals

The algorithm shown in figure 2.2 is valid for analog voice signals. The signal travelling through the wireless communication system is in the digital domain; hence some modification is required to the above approach. The subjective voice quality testing is replaced by measurement of Bit error rate (BER). The BER measurement gives the ratio of the number of bits, which are different between the transmitted frame and the received frame. The pitch detection is also replaced by a separate identification block based on autocorrelation. The signal processing block is connected to the front end of the receiver, so as to minimize the noise component before the decoding and demodulation process at the receiver.

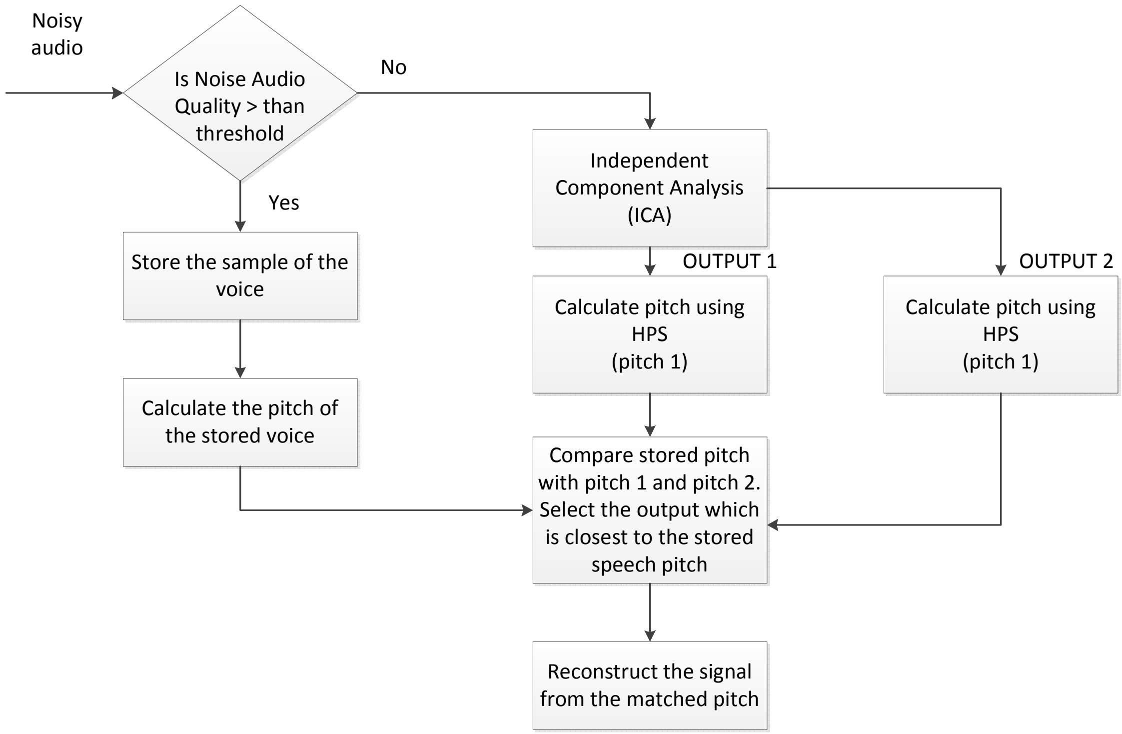

Figure 2.2 Flowchart of initial approach to ICA for call drop reduction [1].

The SPB was first tested for a basic digital communication system similar to GSM system. The system was implemented in Matlab. Basically, frames of 500 random bits were created at the transmitter. The modulation scheme used in the transmitter was QPSK. The system was implemented in a ricean channel with additive white Gaussain noise. At the receiver, channel estimation was carried out by using a phase linear estimator, and then the symbols were demodulated using a hard slicer. The performance analysis was carried out by measurement of bit error rate (BER) with the SPB inserted in the receiver, and without it. A comparison was done between these two BER values for different values of SNR, and a graph of Eb/N0 vs BER was plotted. The result proved that the SPB was able to significantly reduce the BER in the system. The details of the result are given in [1, 2].

CHAPTER 3

THIRD GENERATION WIRELESS COMMUNICATION SYSTEMS

3.1 Introduction

Third generation systems are generally referred to as Universal Mobile Telecommunication System (UMTS) in Europe, and as International Mobile Telephony 2000 (IMT-2000) in USA and Japan. UMTS represents the complete system, including elements such as the user's mobile equipment, the radio infrastructure necessary to support the call or data session, and the core network equipment that is necessary to transfer that user call or data from end to end, as well as billing systems, security systems etc.[5]

3.2 Requirements of Third-Generation Systems

The main requirements for third generation systems are listed below [6] :

- Support of bit rates up to 2 Mbps
- Variable bit rate to offer bandwidth on demand
- Multiplexing of services with different quality requirements on a single connection, e.g. speech, video and packet data
- Delay requirements from delay sensitive real time traffic to flexible best-effort packet data
- Quality requirements from 10% frame error rate to 10^{-6} bit error rate
- Coexistence of second and third generation systems, and inter system handovers for coverage enhancements and load balancing.

3.3 UMTS services

UMTS supports a variety of services. Some of these services are listed below:

3.3.1 Speech

Speech services are probably the oldest services provided by wireless communications technology. UMTS uses the Adaptive Multi-rate (AMR) technique in the speech codec. The Radio Access Network (RAN) chooses the bit rate to be used. The bit rate can be changed after every 20ms speech frame. The Algebraic Code Excited Linear Predictor Coder (ACELP) is used as the coding scheme, where after every 160 speech signals, the parameters of the CELP model are generated from the signal. Discontinuous transmission using Voice Activity Decoder (VAD) helps in prolonging battery life for a user terminal for speech signals. The AMR-narrow band (NB) has a sampling frequency of 8000 samples/sec, while AMR-wideband (WB) uses a sampling frequency of 16000 samples/sec. The wide band solution leads to better voice quality at the expense of additional bandwidth [6].

3.3.2 Messaging

The short messaging service (SMS), picture messaging, multimedia messaging (MMS) are all supported by UMTS. SMS and picture messaging are essentially inherited from the GSM system. MMS is also known as a store and forward messaging, where the message is stored in the server until it is fetched by the receiver. There is no limitation on the delivery time, but only that the message should be delivered to the recipient with high probability. The end user should be able to carry out messaging, while receiving a voice call [6]. Another type of messaging, which is becoming very popular is instant messaging, which enables the users to use chat clients available from Yahoo, MSN, and Google for real time chatting as well as transferring files from their Smartphones.

3.3.3 Video services

Video services include telephony, conferencing, streaming and multimedia gaming. These video services require very low BER and high data rates. Video telephony includes sharing of live video clips between end users during an ongoing voice call. The resolution of the video is highly dependent on the available bit rate, and the video source coding used. Video streaming includes watching live TV channels and other videos available on the internet using smartphones. For real-time multiplayer games, the delay in the system should be as low as possible [6].

3.3.4 Internet Browsing and Mobile Email

Internet browsing should be fast and easily accessible for the end user in different possible environments, with low end to end network delay [6]. Mobile Email is used by clients to access their email using HTML browsers or through an email client already present in the smartphones.

3.4 UMTS Network Architecture

The UMTS uses the same well known architecture that has been previously used by all second generation systems, and are also to some extent, similar to those present in the first generation systems [6]. The network architecture can be grouped into three main parts, viz. the UMTS Terrestrial Radio Access Network (UTRAN), the Core Network (CN) and the User Equipment (UE). The complete block diagram of the UMTS network architecture is shown in figure 3.1.

The details of the network architecture can be found in [6]. We are explaining briefly the working of different elements present in the system in the sections below. Our point of interest is the downlink air interface between the Node B and the User Equipment.

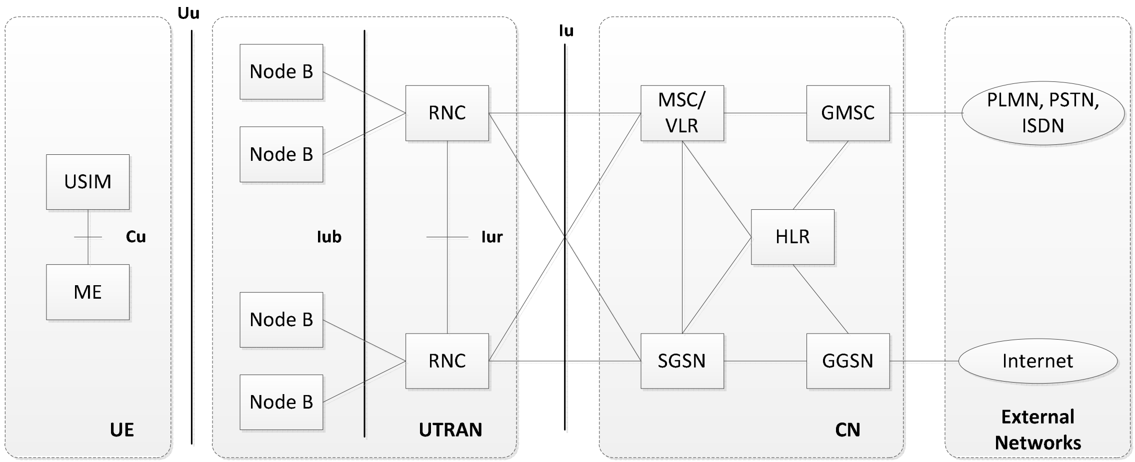

Figure 3.1 UMTS Network Architecture [6].

3.4.1 User Equipment

The User Equipment consists of the Mobile Equipment (ME), and the UMTS Subscriber Identity Module (USIM). Mobile equipment refers to the actual mobile handset used by the consumer to communicate with the UTRAN. USIM is basically a smartcard similar to the Subscriber Identity Module (SIM) used in GSM systems, which contains the subscriber information needed for authentication in the system.

3.4.2 Core Network

The Core network provides connections for both voice calls and data links to external networks. External networks can be circuit switched (CS) or packet switched (PS) networks. CS networks are responsible for connections to ISDN (Integrated Services Digital Network) and PSTN (Public Switched Telephone Network), while PS networks provide data connections to the internet.

The Core Network is not significantly different than the one present for GSM systems, since UMTS technology was built on GSM technology. The main elements of the Core network are listed below:

3.4.2.1 Home Location Register (HLR)

HLR is a database, which stores the main information for the end user, such as the list of services subscribed to by the user, allowed roaming areas, the authorization and security keys specified for the user.

3.4.2.2 Mobile Services Switching Centre/Visitor Location Register (MSC/VLR)

The MSC is a switching node that supports the UE for circuit switched connections [7]. The MSC stores information about the current cell location of the user. When a user moves from one cell to another, while the voice call is in progress, the MSC helps in the handoff process by providing the location of the user to the appropriate RNC's and Node B's. The VLR is a database that stores the current profile of a user. This information is updated continuously as the user moves to different cells.

3.4.2.3 Gateway MSC (GMSC)

The GMSC provides an interface to the external circuit switched networks, and all CS connections are routed through the GMSC.

3.4.2.4 Serving GPRS Support Node (SGSN)

GPRS, which stands for General Packet Radio Service is a mobile data service used in GSM. The SGSN serves as a switching node for packet switched connections. Its function is similar to that of MSC, and it stores the current location of the user, and all incoming packets and outgoing packets from the user are routed through the SGSN.

3.4.2.5 Gateway GPRS Support Node (GGSN)

GGSN provides an interface to external packet switched networks such as the internet. Incoming data packets to the user are forwarded to SGSN using GPRS tunnel protocol [7].

3.4.3 Universal Radio Access Terrestrial Radio Access Network

The UTRAN handles the air interface between the UE and the Node B. The UTRAN consists of Radio Network Controllers and the Node B's connected to them.

3.4.3.1 Node B

A Node B serves the same function as that of a base station in GSM systems, and provides data flow between the UE and the RNC. It also helps in radio resource management functions.

3.4.3.2 Radio Network Controller (RNC)

The radio network controller is responsible for all the radio resources in the different cells associated with it. It performs functions such as handoff, channel allocation and power control. The RNC is connected to the Core Network. It routes CS connections to the MSC, and PS connections to the SGSN.

3.5 Wideband Code Division Multiple Access (WCDMA)

WCDMA is a wideband Direct-Sequence Code Division Multiple Access (DS-CDMA) system, i.e. user information bits are spread over a wide bandwidth by multiplying the user data with quasi-random bits (called chips) derived from CDMA spreading codes [6]. It is the radio technology used in the air interface of UMTS.

Both Time Division Duplex (TDD) and Frequency Division Duplex (FDD) are supported by WCDMA. In TDD, the single 5 MHz carrier is time shared for uplink and downlink, while for FDD two different 5 MHz carriers are used. Coherent detection is used at the receiver, whereby pilot bits are either inserted into the data frame, or transmitted separately using a different physical channel for channel estimation. The main parameters for WCDMA are listed in table 3.1.

Table 3.1 Main WCDMA parameters [6]

Multiple Access Method	DS-CDMA
Duplexing Method	Frequency division duplex/time division duplex
Base station synchronization	Asynchronous operation
Chip rate	3.84 Mcps
Frame Length	10 ms
Service multiplexing	Multiple services with different quality of service requirements multiplexed on one connection
Multirate concept	Variable spreading factor and multicode
Detection	Coherent using pilot symbols or common pilot
Multiuser detection, smart antennas	Supported by the standard, optional in implementation

3.6 Simulation of the physical layer of the UMTS FDD system

The physical layer block diagram for a 3G system is as shown in figure 2.2. The block diagram can be divided into three parts – transmitter, channel and the receiver. The complete block diagram was implemented in Matlab with the signal processing block inserted at the front end of the receiver.

The coding and multiplexing operations carried out in the transmitter, are explained in detail in chapter 4, while chapter 5 is used to explain the spreading and modulation operations for the downlink signal. The channel and noise parameters are discussed in chapter 6. The receiver part is described in chapter 7.The results of the simulation results are listed in chapter 9.

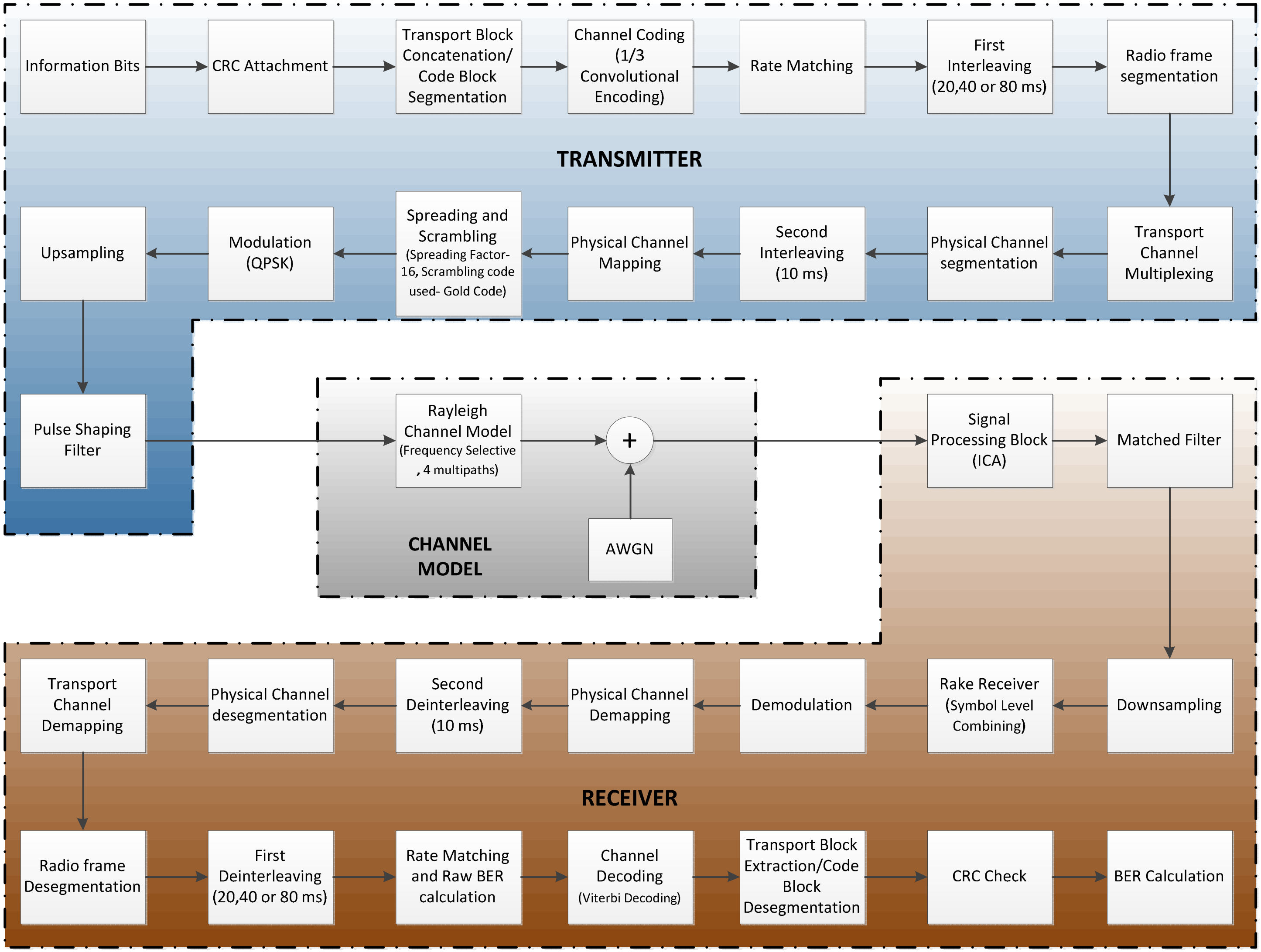

Figure 3.2 Complete Physical layer block diagram of a 3G wireless communication system with signal processing block (SPB).

CHAPTER 4

SIMULATION OF TRANSMITTER SECTION -CODING AND MULTIPLEXING

4.1 Coding and Multiplexing

The multiplexing and coding chain for the downlink operation on the transmitter side is shown in figure 4.1. Each of the blocks is explained in the following sections.

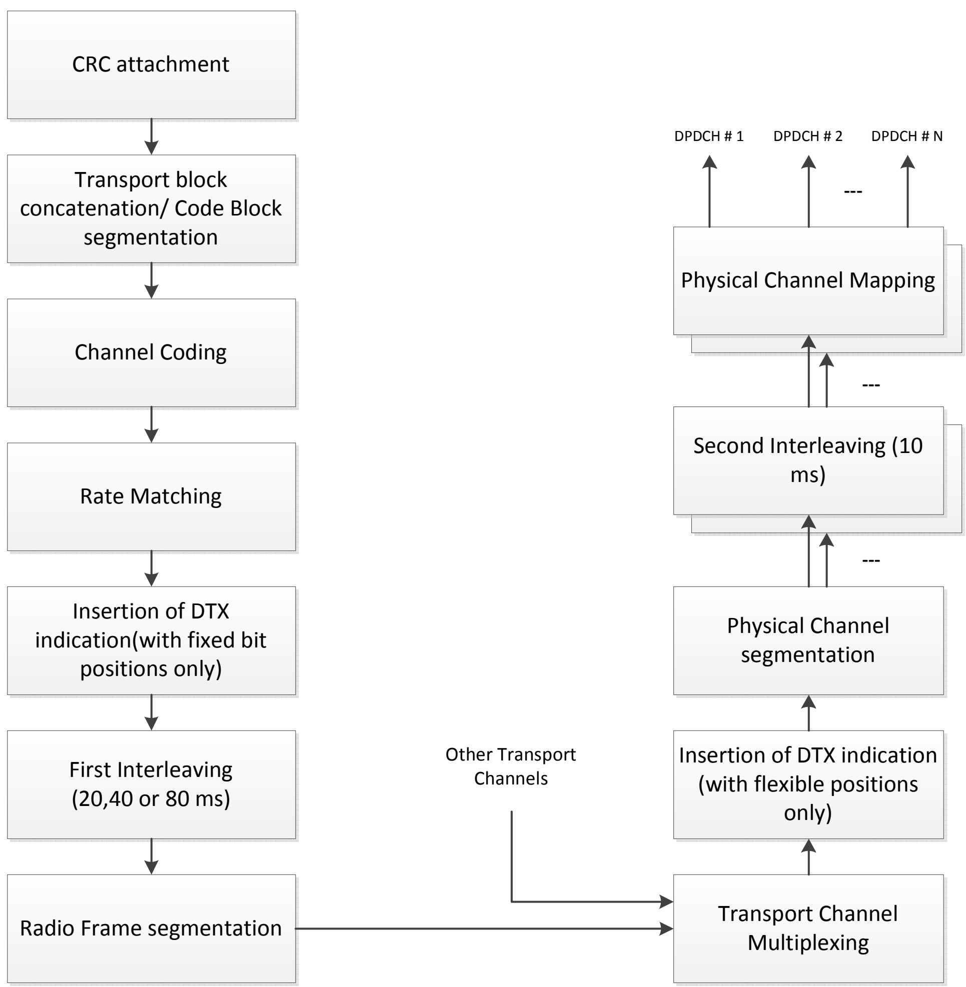

Figure 4.1 Downlink multiplexing and channel coding chain [6]

4.2 Generation of Information Bits

The information bits for both the transport channels (DCH1 and DCH2) used in the simulation are randomly generated in Matlab using the function ‘randsrc’. These information bits take the value ‘1’ or ‘0’ with a probability of 0.5. We choose a payload length of 244 bits for the data channel and a length of 100 bits for the control channel.

4.3 CRC (Cyclic Redundancy Check) Attachment

CRC parity bits are appended to the data being transmitted for the purpose of error detection. The more the number of CRC bits, less is the probability of error [6]. Figure 4.3 shows an example of CRC bits being added on to data blocks transferred from the MAC (Medium Access layer) onto the transport channel.

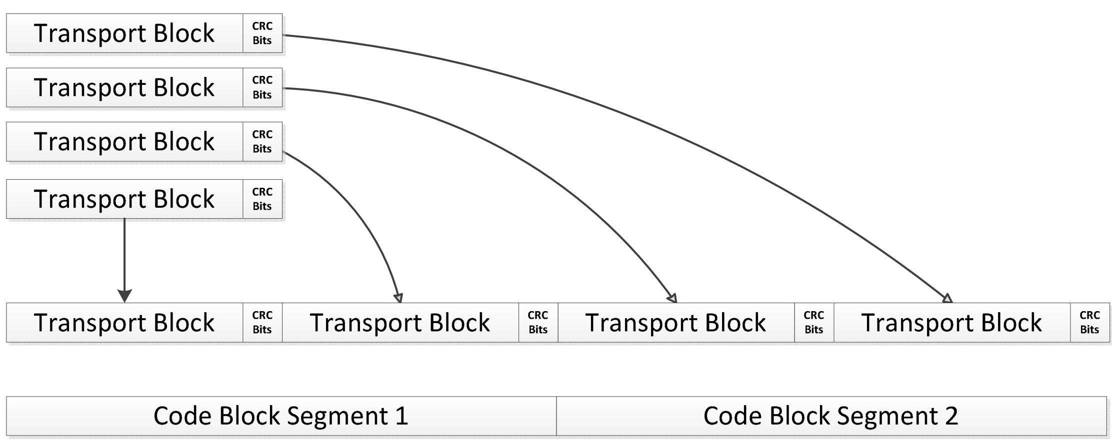

Figure 4.2 Example of CRC attachment and code block segmentation [5].

The parity bits are generated by one of the following cyclic generator polynomials:

$g_{CRC24}(D) = D^{24} + D^{23} + D^{6} + D^{5} + D + 1;$

$g_{CRC16}(D) = D^{16} + D^{12} + D^{5} + 1;$

$g_{CRC12}(D) = D^{12} + D^{11} + D^{3} + D^{2} + D + 1;$

Figure 4.4 shows the general form of an encoder used in WCDMA. First the set of data bits are transmitted, and then the switch is shifted to the down position for the transmission of parity bits. This is followed for all the transport blocks. The decoding is done by dividing the blocks, with the same polynomial used at the transmitter side. The decoder also has similar shift register architecture as that of the transmitter [5].

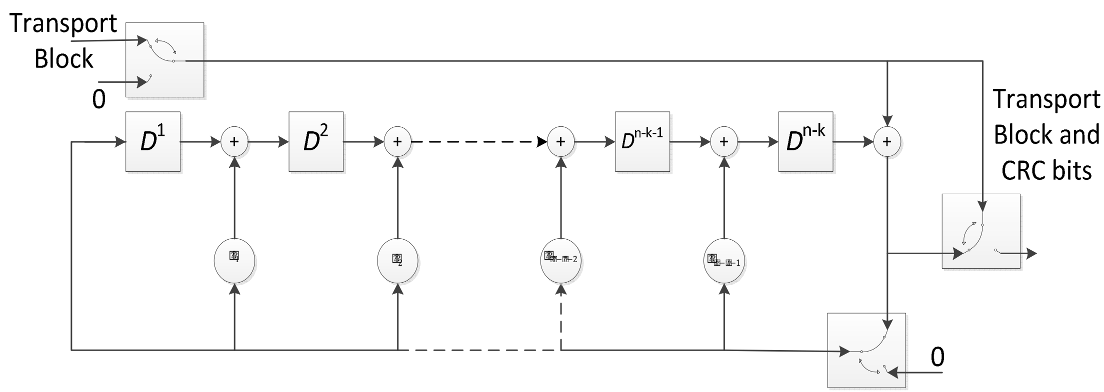

Figure 4.3 General Form of the encoder [5].

For the UMTS configuration, 18 bit and 12 bit CRC generator polynomials are used for the data and control blocks respectively. For the HSDPA configuration, 24-bit CRC generator polynomial is used.

4.4 Transport Block concatenation and code block segmentation

Transport block concatenation refers to combining together the transport blocks that belong to the same transport channel. Code block segmentation refers to the segmentation of a given block into smaller blocks, when the transport block exceeds the size limitation set by the type of channel coding chosen. For example, convolutional coding has a maximum block size of 504 bits, while turbo coding has the size set to 5114 bits. If the transport blocks are not of the same size after segmentation, filler bits are added to the first segmented block [13]. In the

Matlab simulation, segmentation is not required because the size of both the data and the control blocks are both less than 504 bits.

4.5 Channel Coding

Channel coding is used to mitigate the effects of the harsh radio environment such as fading of the information bits when the signal is transmitted from the base station to the user equipment. Coding techniques are classified as block coding and convolutional coding. Block coding consists of appending parity bits to information bits in blocks to form a codeword, while convolutional coding acts on continuous data streams to construct the code words.

4.5.1 Convolutional Codes

Convolutional codes were first put forward by P. Elias in the paper ‘Coding for noisy channels’ published in 1955 [8]. The encoder is generally implemented using shift registers and modulo-2 adders, while the decoding is performed using the Vitterbi algorithm.

4.5.2 Convolutional Encoder

The Convolutional encoder consists of shift registers and modulo-2 adders. The information bits are fed into the registers one bit at a time for binary symbols. The contents of the shift registers are added together using modulo-2 adders to produce the outputs. The number of shift registers is known as the constraint length of the encoder. The taps going to the modulo-2 adders are decided based on the generator polynomial used. If the input data symbols are ‘k’ bits and output codeword’s are ‘n’ bits in size then the coding rate is defined as ‘k/n’. The codeword’s are also referred to as (n, k, l) codes where n and k are the length of the input and corresponding output bits and l stands for constraint length [5].

For example, consider a 1/3 rate convolutional encoder with constraint length equal to three as shown in the figure 4.4. The modulo-2 taps are decided by using the generator polynomial ‘g’.

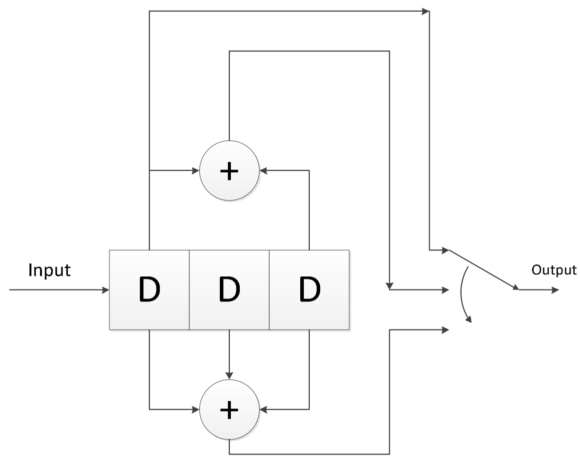

Figure 4.4 Basic structure of 1/3 rate convolutional encoder [5].

The working of the encoder can be defined using state diagrams, which map the changes in the values of the shift registers with the application of each input bit. The shift registers represent the memory storage components of the encoder. For an encoder with constraint length ‘L’, there are $L-1$ bits in the memory. In this case there are 2 bits in memory of the encoder. The state diagram for the above $(3,1,3)$ codes is shown in Figure 4.5.

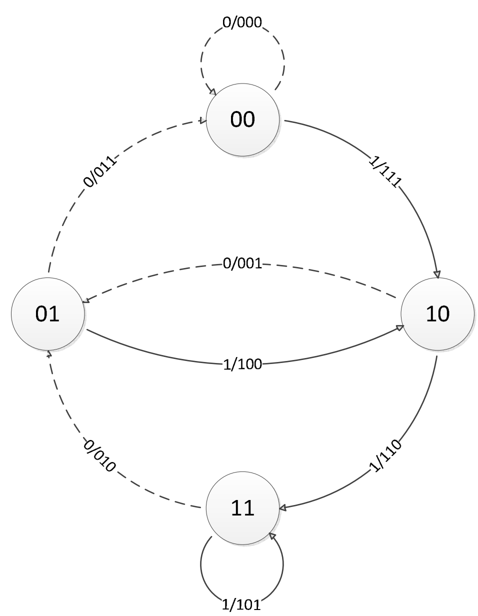

Figure 4.5 State Diagram for (3, 1, 3) Code [5].

The state diagram is then converted into a trellis structure which represents the various possible transitions that occur between the states depending on whether the input bit is binary ‘0’ or ‘1’. From a particular state, there are only two possible paths towards the next state. The dashed lines represent an input of ‘0’, whereas the solid lines represent an input of ‘1’.The trellis structure is shown below in Figure 4.6.

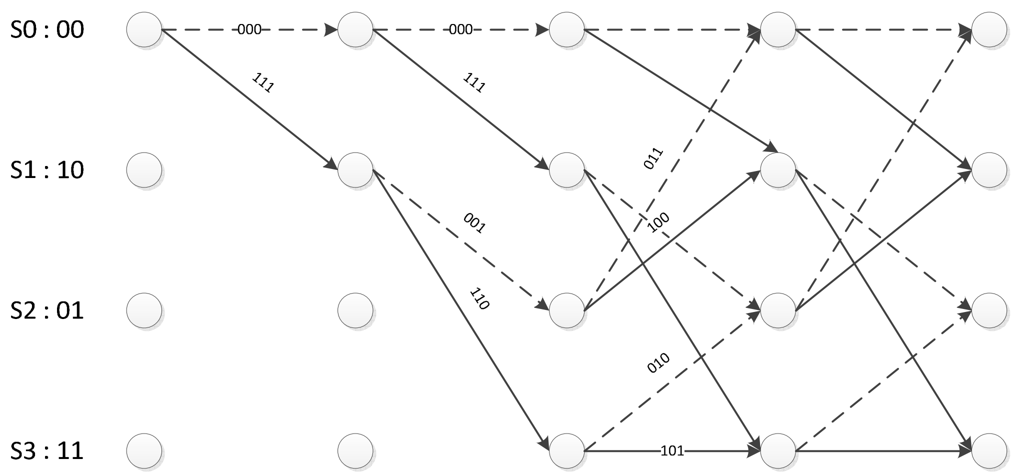

Figure 4.6 Trellis structure for (3, 1, 3) code [5].

Since convolutional encoding works on continuous streams of data, it should be terminated to a known state at the end of transmission for the receiver to accurately decode it. For this purpose, tail bits are appended to the transmission bits to end the trellis structure at state ‘0’.

4.5.3 WCDMA convolutional codes

In WCDMA, the two commonly used convolutional encoders are shown in Figure 4.7. The first encoder is ½ rate, which indicates that there are two output bits for every input bit. It has a constraint length of 9 with 8 shift registers. The second encoder is 1/3 rate and has the same number of shift registers.

For both the encoders, eight tail bits are added to the transmitted bits to ensure proper decoding at the receiver. The second encoder has been used in our Matlab simulations.

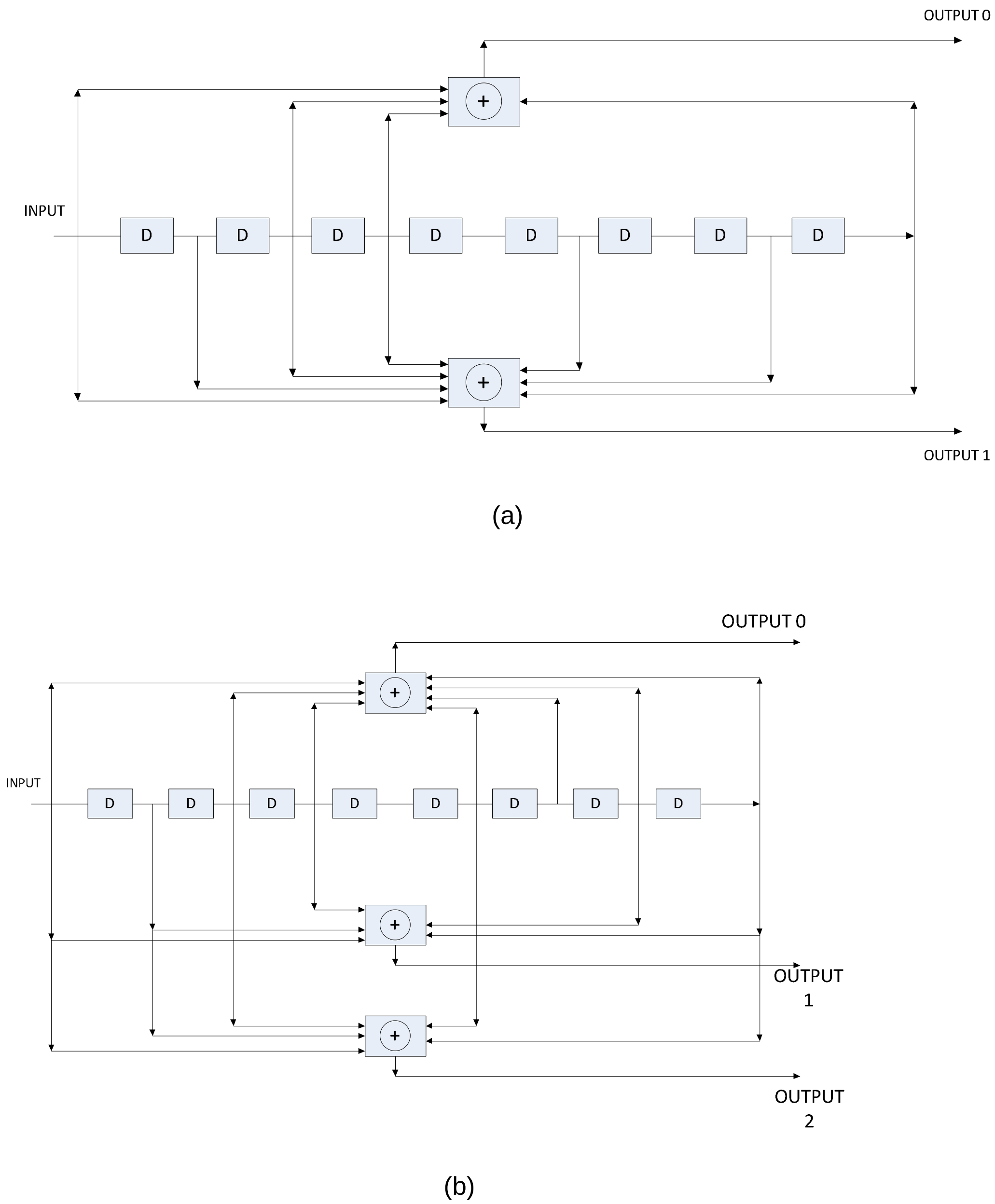

Figure 4.7 Examples of WCDMA convolutional encoder (a) ½ rate encoder (b) 1/3 rate encoder [5]

4.6 Rate Matching

The rate matching operation is carried out to match the data rates required by different blocks of data sent from the higher layers. The number of bits on a transport channel can vary between different transmission time intervals. There are two ways to carry out rate matching either by using fixed bit positions or flexible bit positions.

When fixed bit positions are used, it means that the same symbols are used in the transport channels. If the transmission rate is less than the maximum, then DTX (Discontinuous indication bits) are inserted into the slot positions as shown in figure, to inform the transmitter at which bit positions the transmission should be turned off [6]. On the other hand, if the transmission rate is too high, then puncturing is carried out.

When flexible bit positions are used, puncturing or insertion of DTX bits is carried out once all of the data to be transmitted within a radio frame is assembled [5]. This is useful since the bits in the slot, which are unused by one application can be utilized by another application. Figure 4.8 shows the rate matching operation using fixed and flexible bit positions for two transport channels 'A' and 'B'.

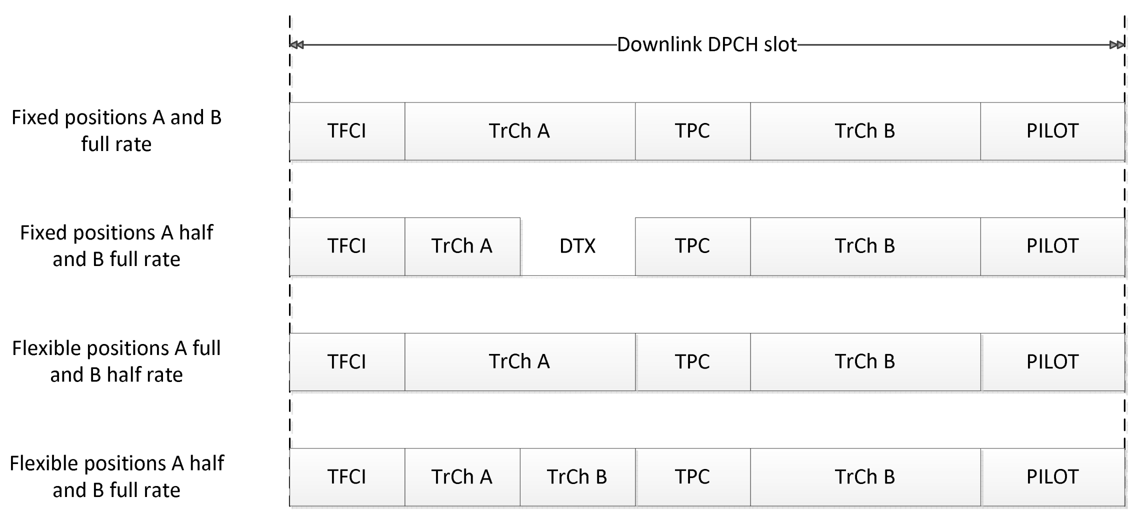

Figure 4.8 Flexible and fixed transport channel slot positions in the downlink [6]

In our case, we consider a flexible scenario, where both the data blocks in the slots are used by the same transport channel.

4.7 First Interleaving

The first interleaver is a block interleaver which performs inter-column permutations. The block interleaver reduces the effect of burst errors, those lasting many bits, as might result from a mobile undergoing a severe fade, when the signal travels through the channel [9]. The bits are first read into a matrix, whose columns are defined according to the transmit time interval (TTI). Once the data is read into the matrix, then intercolumn permutations are carried out according to the table 4.1. In our case, we consider a TTI of 10 ms, hence only a row to column interleaving takes place without any permutations.

Table 4.1 Inter-column permutation patterns for 1st interleaving [13]

TTI	Number of columns C1	Inter-column permutation patterns
10 ms	1	<0>
20 ms	2	<0,1>
40 ms	4	<0,2,1,3>
80 ms	8	<0,4,2,6,1,5,3,7>

4.8 Radio Frame Segmentation

When the transmission time interval is longer than 10 ms, the input bit sequence is segmented and mapped onto consecutive equal sized radio frames. In our case, for (Dedicated channel) DCH1, the 540 bits in the data block are equally divided into two frames of 270 bits, whereas for DCH2, the 240 bits are equally divided into 4 frames of 60 bits each.

4.9 Transport Channel Multiplexing

Every 10 ms, one radio frame from each transport channel (TrCH) is delivered to the multiplexing block. These radio frames are serially multiplexed into a coded composite transport channel (CCTrCH). In the Matlab simulation, the two different transport channels (DCH1 and DCH2) are combined in this block. The process involves combining 270 bits from DCH1 and 60 bits from DCH2 to form blocks of 390 bit DPCH frame. The DPCH frame is further divided into 15 slots each. The slot and frame structure for the downlink DPCH is as shown below in figure 4.9.

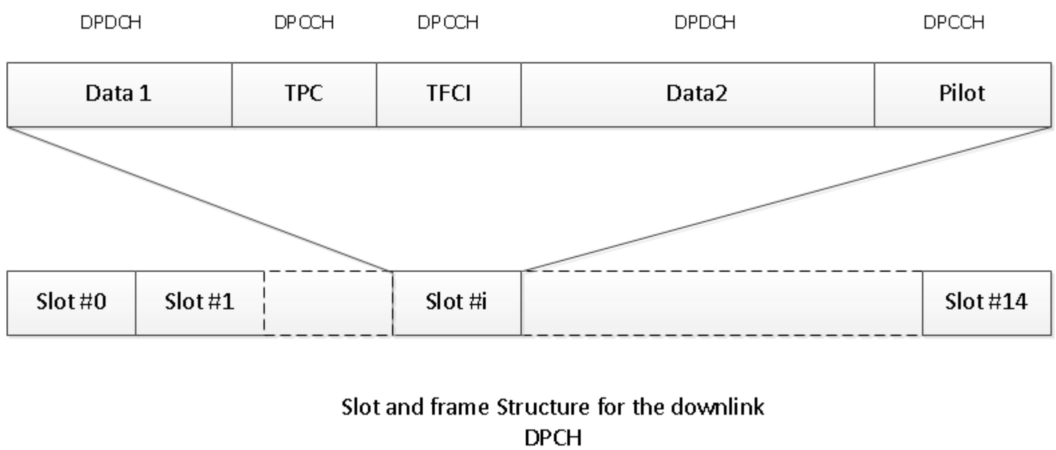

Figure 4.9 Slot and frame structure for the downlink DPCH [6]

4.10 Physical Channel Segmentation

If multiple physical channels are present, then physical channel segmentation divides the data in the composite transport channel among these channels. .

A summary of the above operations is illustrated in figure 4.10.

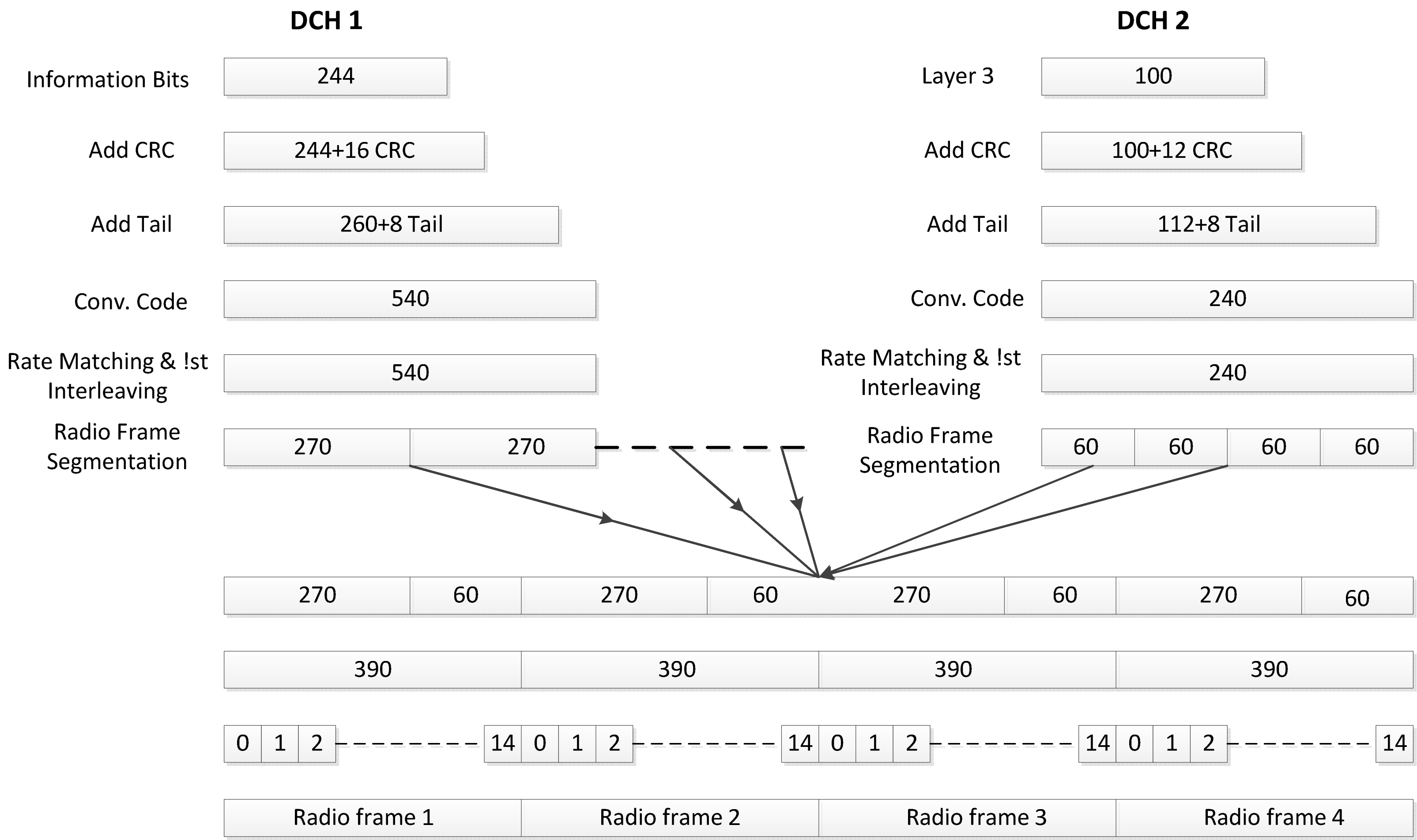

Figure 4.10 Coding and Multiplexing simulation example [5]

4.11 Second Interleaving

The second interleaver is a block interleaver, which performs inter-column permutations. The data is first read into a matrix with 30 columns. Padding is carried out if the number of data is not a multiple of 30. After this step, inter-column permutations are carried out according to table 4.1. It operates on frames of 10 ms each.

Table 4.1 Inter-column permutation pattern for 2nd interleaving [13]

Number of columns	Inter-column permutation pattern
30	<0, 20, 10, 5, 15, 25, 3, 13, 23, 8, 18, 28, 1, 11, 21, 6, 16, 26, 4, 14, 24, 19, 9, 29, 12, 2, 7, 22, 27, 17>

4.12 Physical Channel Mapping

In the UMTS system, the data from the higher layers is carried over the air interface in transport channels, which are mapped onto different physical channels [6]. To understand the different physical channels, we must first understand the different transport channels present in the system.

The transport channels are classified into two types: dedicated transport channels (DCHs) and common channels. The dedicated channels are unique to the user, while common channels are shared between different users. A detailed explanation of the transport channels is given in [6].

4.12.1 Dedicated Transport Channel

The dedicated transport channel is used to carry the entire information specific to the user. It also carries control information from the higher layers intended for the user. It has features such as fast power control, variable data rate etc.

4.12.2 Common Channels

The different common channels include [6]

Broadcast channel (BCH): The broadcast channel as the name suggests is used to broadcast information throughout the cell. This information includes available channelisation codes, slots available, type of transmit diversity etc.

Forward Access Channel (FACH): This channel is used to send control information to the user terminal. It is generally used to acknowledge a reply after receiving a request from the user terminal. The FACH can also be used for packet data transmission.

Paging Channel (PCH): Paging channel is used to communicate by the Node B with the user terminal. For example, when a call is received by the system for a particular user terminal in a cell, communication is initiated by Node B through the paging channel.

Reverse Access Channel (RACH): RACH is used to carry control information during uplink transmission. For example, when the user wants to make a call, RACH is used by the user terminal to communicate with the system.

Uplink Common Packet Channel (CPCH): The CPCH can be used to carry packet data in the uplink direction. It is basically the same as RACH but can make use of fast power control.

Downlink Shared Channel (DSCH): The DSCH is used to carry user information in the downlink. It is a shared channel and can make use of fast power control, variable bit rate and transmit diversity schemes. In HSDPA, this channel was replaced by High Speed-DSCH (HS-DSCH).

4.12.3 Mapping of Transport channels to Physical channels

The table 4.2 shows the mapping of the transport channels to the physical channel. Some physical channels carry only physical layer information and are not related to any transport channels.

Table 4.2 Transport Channel to Physical Channel mapping [6]

Transport Channels	*Physical Channels*
BCH	Primary Common Control Physical Channel (PCCPCH)
FACH PCH	Secondary Common Control Physical Channel (SCCPCH)
RACH	Physical Random Access Channel (DPCCH)
DCH	Dedicated Physical Data Channel (DPDCH) Dedicated Physical Control Channel (DPCCH)
DSCH CPCH	Physical Downlink Shared Channel (PDSCH) Physical Common Packet Channel (PCPCH) Synchronization channel (SCH) Common Pilot Channel (CPICH) Acquisition Indication channel (AICH) Paging Indication channel (PICH) CPCH Status Indication Channel (CSICH) Collision Detection/ Channel Assignment Indicator Channel (CD/CA-ICH)

4.12.4 Downlink Dedicated Channel

The downlink dedicated channel (DCH) is mapped to the Downlink Dedicated Physical Channel (DPCH). There are in reality, two physical channels present: Dedicated Physical data Channel (DPDCH), which contains the user information and Dedicated Physical Control Channel (DPCCH), which contains control information from the higher layers. In the downlink, both these channels are time multiplexed into a single Downlink Dedicated Physical Channel (DPCH) frame as shown in the Figure 4.9. The pilot bits present in the DPCCH can be used for channel estimation at the receiver.

4.12.5 Common Pilot Channel (CPICH)

The CPICH is a known un-modulated data sequence with a pre-defined channelisation code and scrambling code which can be used by the receiver for channel estimation. It is generally a sequence of complex $(1 - j)$.

In this chapter, we have explained the coding and multiplexing operations, carried out in the transmitter of a UMTS system. These operations form a part of the transport layer operations. The next chapter is used to explain the physical layer operations taking place in the transmitter such as spreading, scrambling and modulation.

CHAPTER 5

SIMULATION OF TRANSMITTER SECTION - SPREADING AND MODULATION

Spreading is the fundamental property associated with wideband code division multiple access technique. There are two types of spreading codes used: channelisation codes and scrambling codes. These codes serve different functions in uplink and downlink.

5.1 Channelisation codes

The basic unit in WCDMA is the chip, which is a portion of the bit to be transmitted, whose width depends on the length of the channelisation code. Channelisation codes are short length chip sequences, which are multiplied to the data bits to produce a stream of data chips, which are then transmitted through the air interface. The transmission rate is defined by chips per second. The length of the channelisation codes is known as the spreading factor. Multiplication by channelisation codes increases the bandwidth of the signal in proportion with the spreading factor.

In the downlink, channelisation codes are used to separate the user terminals from each other, while in the uplink, these codes are used to separate the different physical channels from the same user. In WCDMA, the channelisation codes are generated from the Orthogonal Variable Spreading Factor (OVSF) codes. The OVSF code tree is as shown in figure 5.1. The OVSF code tree helps to choose codes with different spreading factors, but at the same time these codes are orthogonal to each other [6]. There are some rules governing the selection of channelisation codes from the OVSF tree. Once a code is chosen from one of the branches of the tree, any codes present in the parent branch or in the overlying branches cannot be chosen.

This is due to the fact that these codes will not be orthogonal to each other. The orthogonality principle is used by the receiver to separate signals from multiple users or multiple antennas.

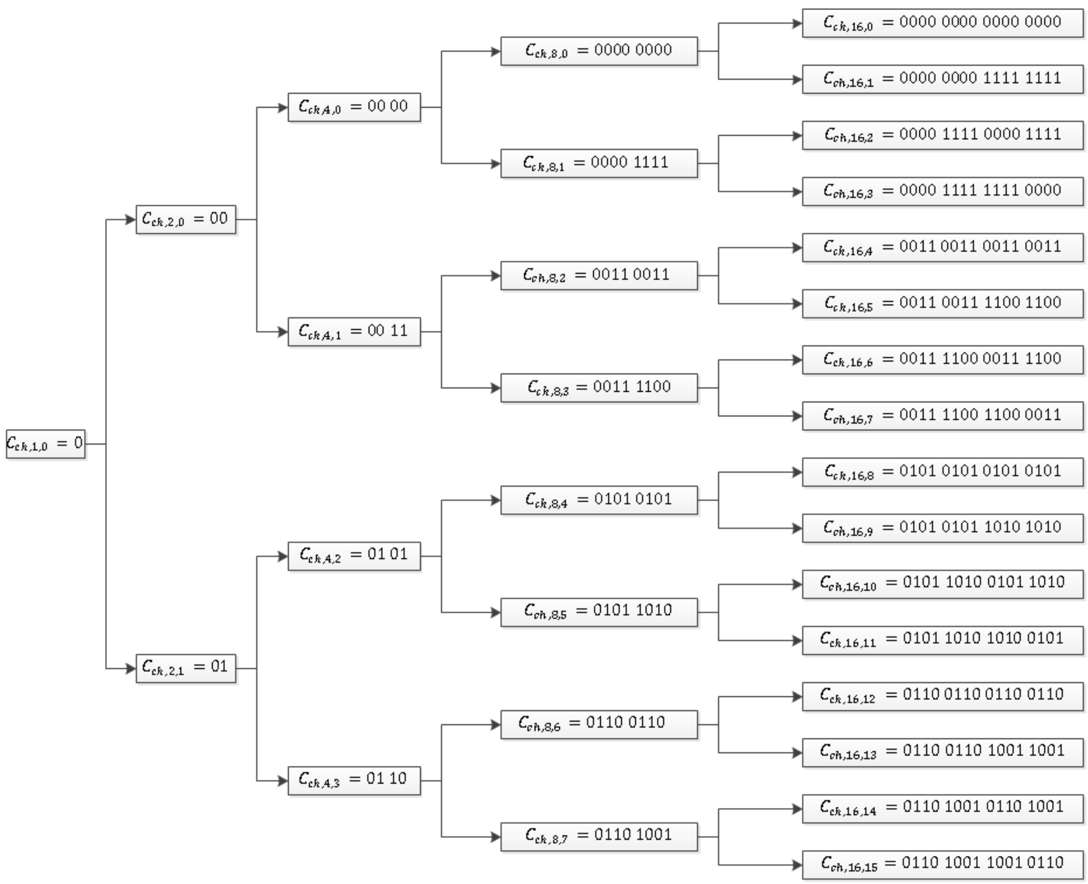

Figure 5.1 OVSF Code Tree [6]

Different data rates are supported by the WCDMA system by choosing different length channelisation codes. The chip rate is fixed at 3.84 Mcps for a WCDMA system, hence by choosing different spreading factors, we can get different data rates. The different possible data rates for a WCDMA system with QPSK modulation are shown in table 5.1.

Table 5.1 Downlink data rates [5]

Code Length	*Example downlink data rate*	*WCDMA downlink data rate*
4	960 kb/s	1.92 Mb/s
8	480 kb/s	960 kb/s
16	240 kb/s	480 kb/s
32	120 kb/s	240 kb/s
64	60 kb/s	120 kb/s
128	30 kb/s	60 kb/s
256	15 kb/s	30 kb/s
512	7.5 kb/s	15 kb/s

The data rates can be easily changed by choosing the appropriate length of the channelisation code. For example, in figure 5.2, when we choose a spreading factor of four, the data rate is 960 kB/s. In the second case, when we choose a spreading factor of eight, the data rate reduces to 480 kB/s, and in the third case with a spreading factor of eight, the data rate further reduces to 240 kB/s. Thus, we can choose the data rate needed for a particular application by changing the code length, also known as the spreading factor. For the WCDMA system with QPSK modulation, the data rate is doubled for each case, since each symbol contains two bits. However, the chip rate in all cases is fixed at 3.84 Mcps.

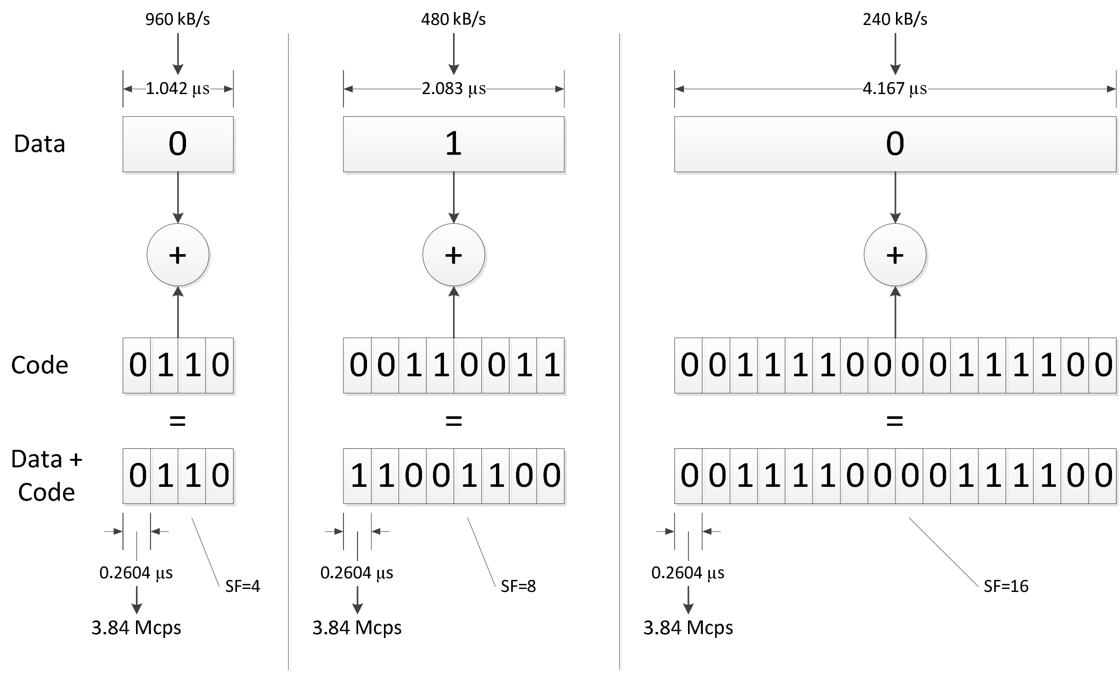

Figure 5.2 Effects of code rate on data length [5]

5.1.1 Single User Spreading and De-spreading

Consider an example, where a single user is present in a single cell. Figure 5.3 illustrates the application of a channelisation code to a data sequence sent form the Node B to the User Equipment. At first, the input sequence is repeated to form the same number of chips as present in the channelisation code. Then the data sequence and the channelisation code are exclusive OR'd together to form the set of chips to be transmitted. The symbol length is increased by a factor of the code length as compared to the original bit. The transitions in the spread data are much higher than those in the original bit sequence giving rise to a larger bandwidth [5]. The chip rate of the transmitted data is fixed at 3.84 Mc/s.

Ignoring the effects of channel and noise, the received chip sequence at the receiver is de-spread by adding it with the same channelisation code using an exclusive OR gate. The dispreading operation is as shown in figure 4.3. It is assumed that the transmitter and receiver have perfect synchronization.

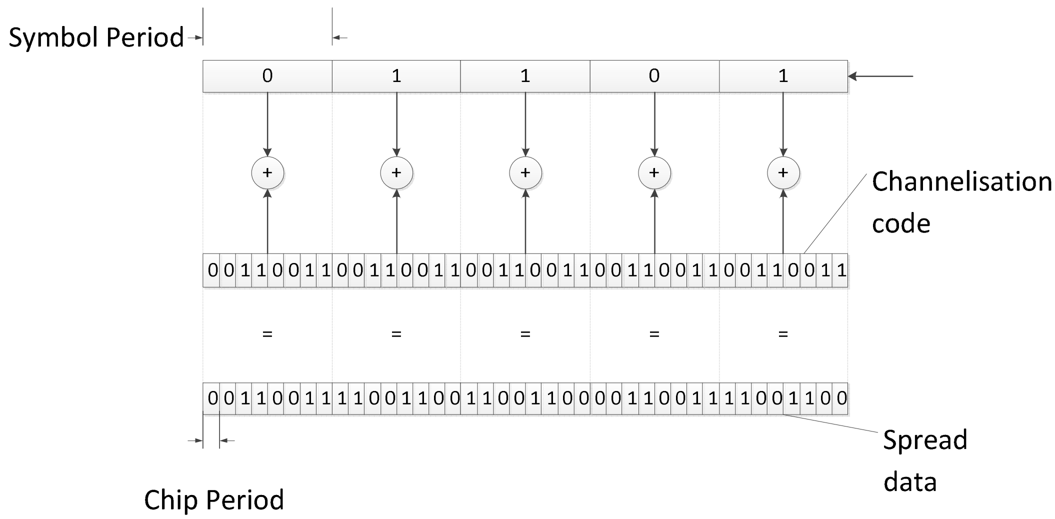

(a)

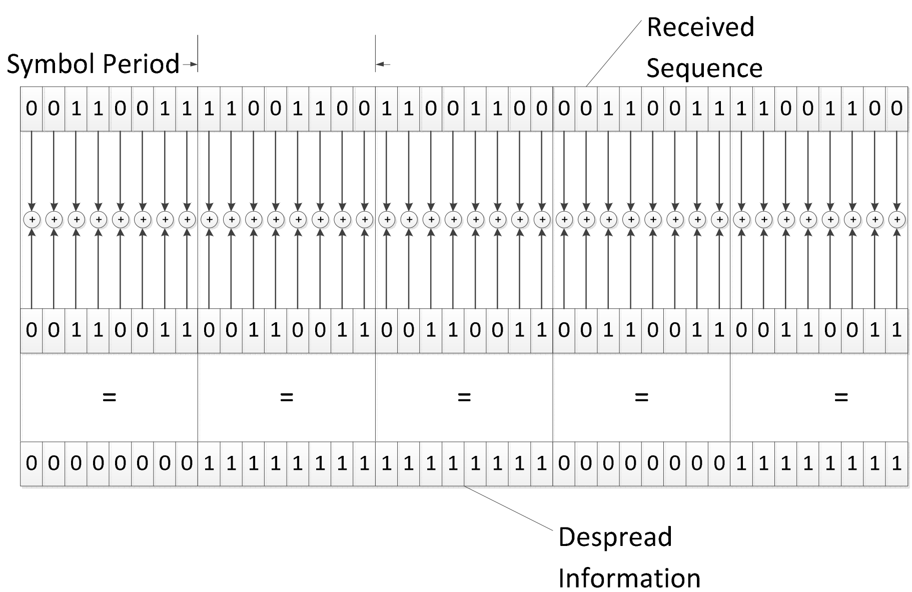

(b)

Figure 5.3 Spreading and De-spreading operation example for single user (a) Spreading (b) De-spreading [5]

5.1.2 Multiple User spreading and De-spreading

In case of multiple users, each user is assigned a particular channelisation code. The data sequences from each of the users are multiplied with the user specific channelisation code. Both the user sequence and the channelisation code are mapped to the polar format before the multiplication. According to the mapping defined by 3GPP specifications, a binary '0' maps to '+1' and a binary '1' maps to '-1'. The result of the multiplication operation produces multiple chips sequences. Figure 5.4 shows the spreading operation for two users. It is assumed that the transmitter and receiver are perfectly synchronized. These polar chip sequences are then added together before transmission. The added signal shows random amplitude variation and cannot be defined as a binary or polar signal [5].

At the receiver, de-spreading operation takes place by multiplying the received chip sequence by the user specific channelisation code. Figure 5.4 b) shows the dispreading operation for two users. In the downlink, at the user terminal, we need to know only the channelisation code of that user to decode the information from the received chip sequence. The information bits for the second user in the received chip sequence are discarded. After multiplication, the decoded chip sequence is passed through a summer or integrator. The function of the integrator is to collect the chip energy across a symbol period. For the example, in figure 5.4, the symbol period is equal to eight chip periods and hence the values of all the eight chips are added to form a single symbol. Then the symbol is detected at this point, and the integrator is reset. A processing gain equal to the spreading factor i.e the length of the channelisation code is obtained after the integration of the chips.

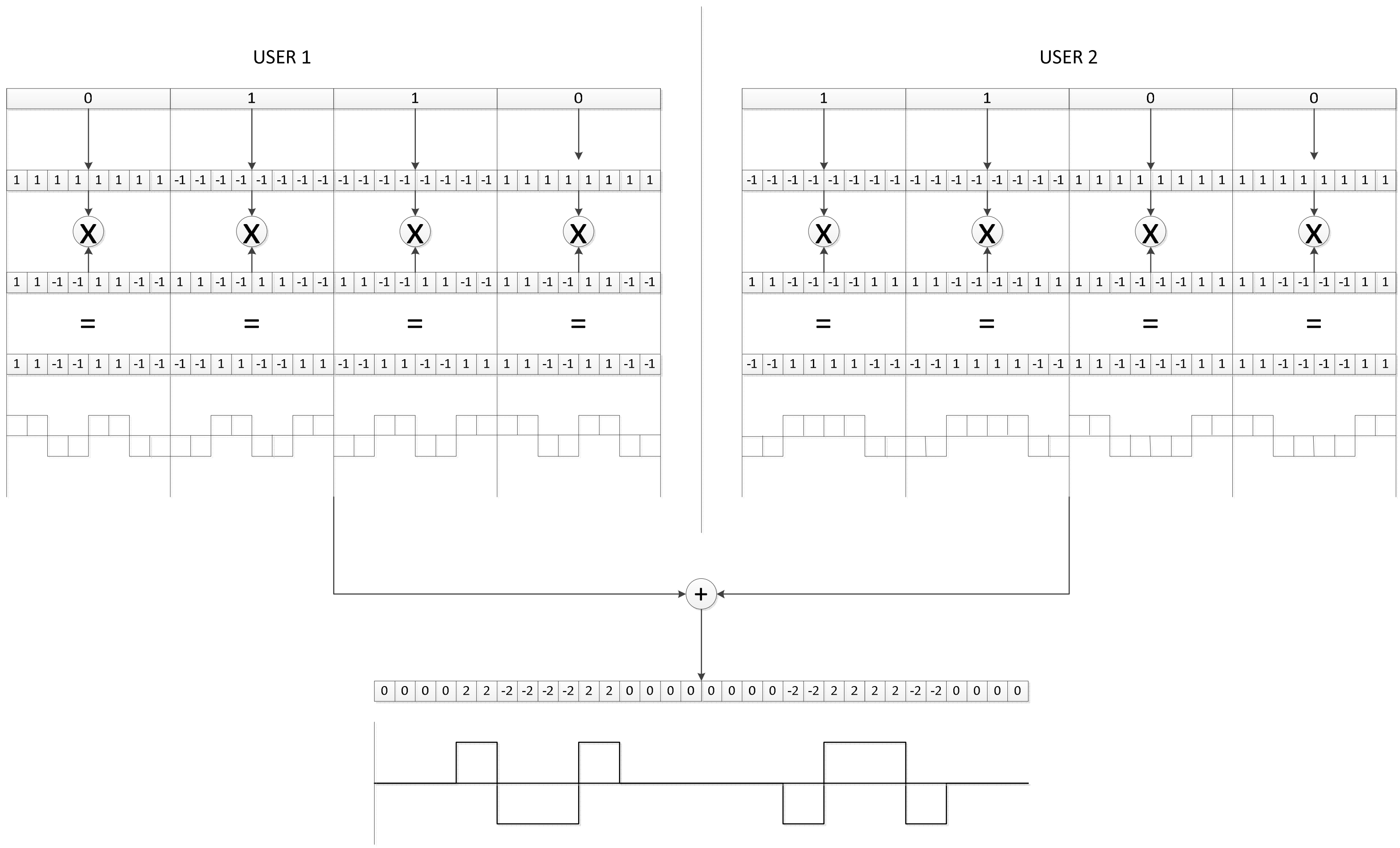

Figure 5.4 Spreading operations for two users

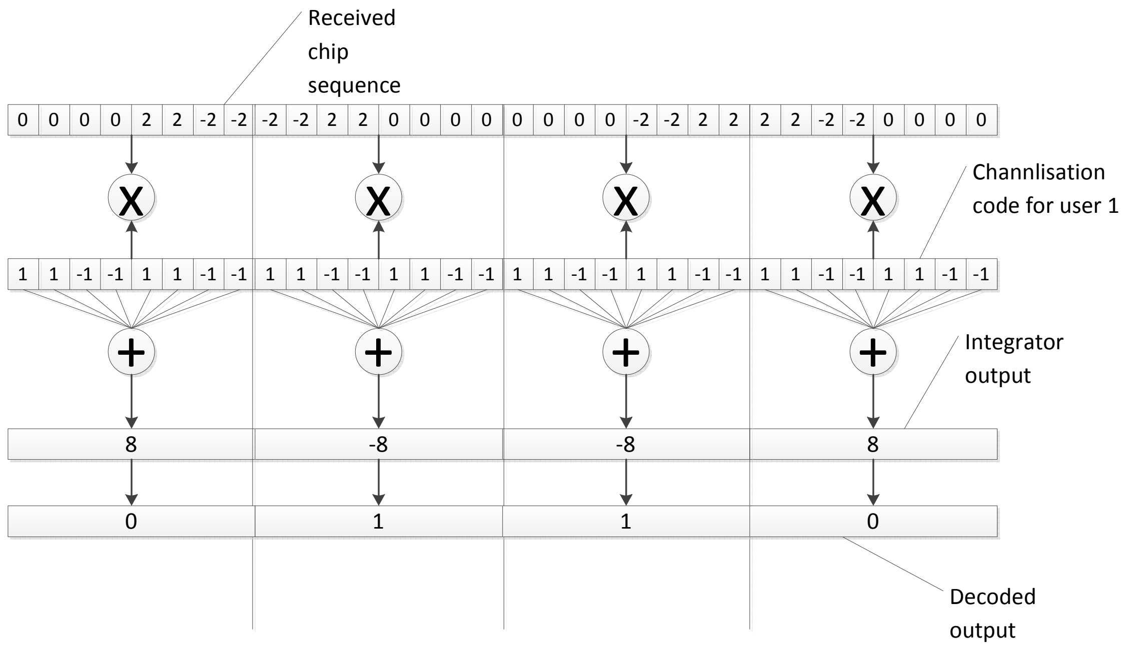

Figure 5.5 De-spreading operation for user 1 [5]

5.2 Scrambling Codes

The scrambling codes are long codes generated from Pseudo Noise (PN) sequences. These codes serve different functions in the uplink and the downlink. In the uplink, the scrambling codes are used to differentiate between the different user terminals, while in the downlink they are used to mitigate inter-cell interference. We will be mainly focusing on the downlink part. Once the spreading factor is fixed, there are only a limited number of available channelisation codes. For example, if a spreading factor of eight is chosen, then from the OVSF tree in figure 5.1, only eight different codes are available. These codes are insufficient to be used by all the cells surrounding the current cell, and hence cannot be used to provide the needed buffer between the different signals originating from the Node B's located in the other cells. Hence to reduce this intercellular interference, the signal to be transmitted is multiplied by another chip sequence known as scrambling codes. The number of available scrambling codes in the downlink is fixed at 512. Anything larger than this number would result in a cumbersome cell search procedure. The scrambling code to be used in the cell is decided by the UTRAN. The multiplication of the scrambling code does not have any effect on the bandwidth of the signal as illustrated from the figure 5.6.

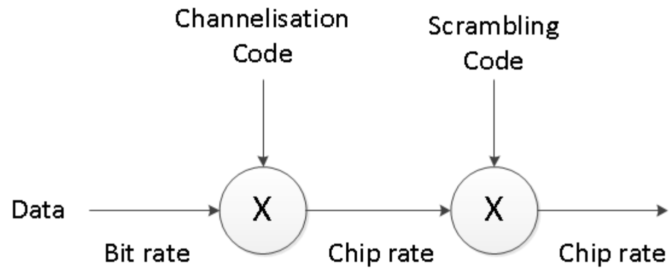

Figure 5.6 Relation between spreading and scrambling [6]

The scrambling codes generally should have large autocorrelation values, when the sequences are perfectly aligned, and very low values, when the sequences are not. This property is used extensively in the rake receiver to discard the delayed version of the signal, which occurs outside a chip interval for a particular rake finger. Also the scrambling codes should have low cross-correlation with each other so as to discard the interference signal from another Node B.

In WCDMA, the complex valued scrambling code is formed from a single Gold code by simply having a delay between the 'I' and 'Q' branches. An eighteen degree code generator consisting of shift registers and adders as shown in figure 5.7 is used to generate the code. There are eighteen shift registers in each of the two Gold code generators. The number of possible scrambling codes that can be generated using this configuration is $2^{18} - 1$, of which only 512 codes are used. The upper shift registers are initialized to seventeen binary zeros and a single one at the end. The lower shift registers have all elements initialized to one's.

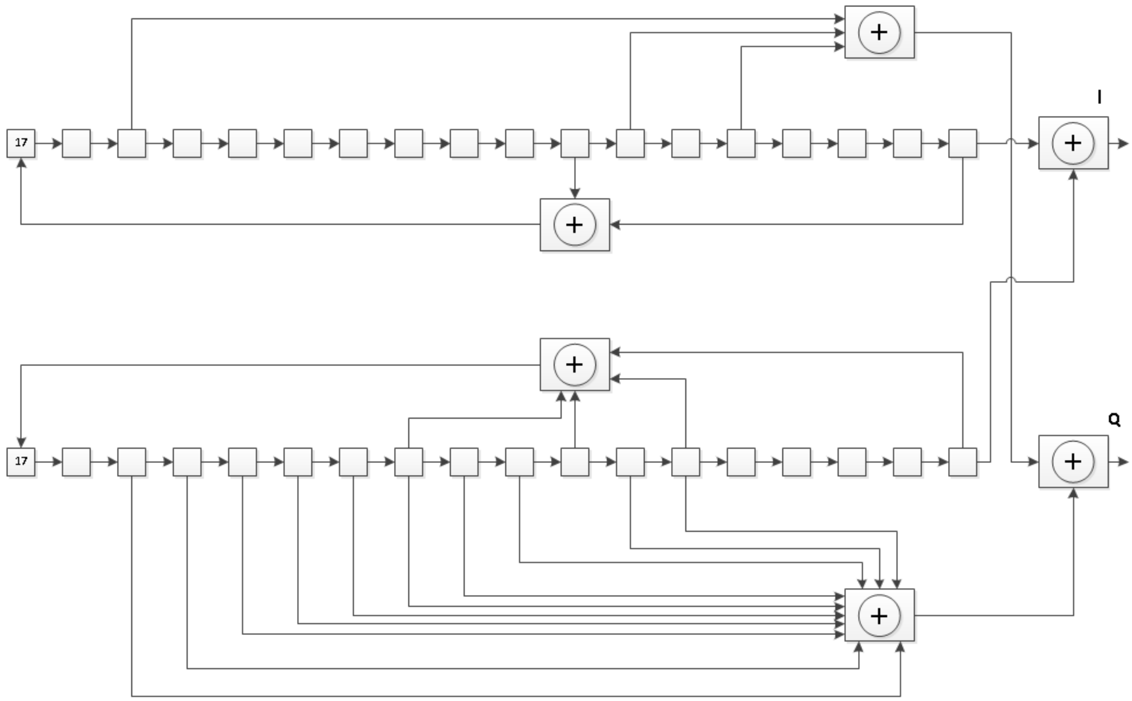

Figure 5.7 Downlink Gold code generator [5]

5.3 Downlink Spreading, Scrambling and Modulation

The bits arriving on the DPCH (Dedicated physical channel) are first converted to polar format by mapping '0' to '+1' and '1' to '-1'. This polar sequence is then passed through a serial to parallel converter, which gives rise to two separate streams of data. The first stream is called the in-phase component, and the second stream is known as the quadrature-phase component. Both the streams are then multiplied with the appropriate channelisation code, which is the same for both the streams. The in-phase stream is multiplied by an RF carrier (cosine waveform) and the quadrature phase stream is multiplied by the same carrier rotated through 90 degrees (sine waveform). The two phase component streams are then added chip by chip to construct the QPSK (Quadrature Phase Shift Keying) symbols [5]. Figure 5.8 illustrates the above process.

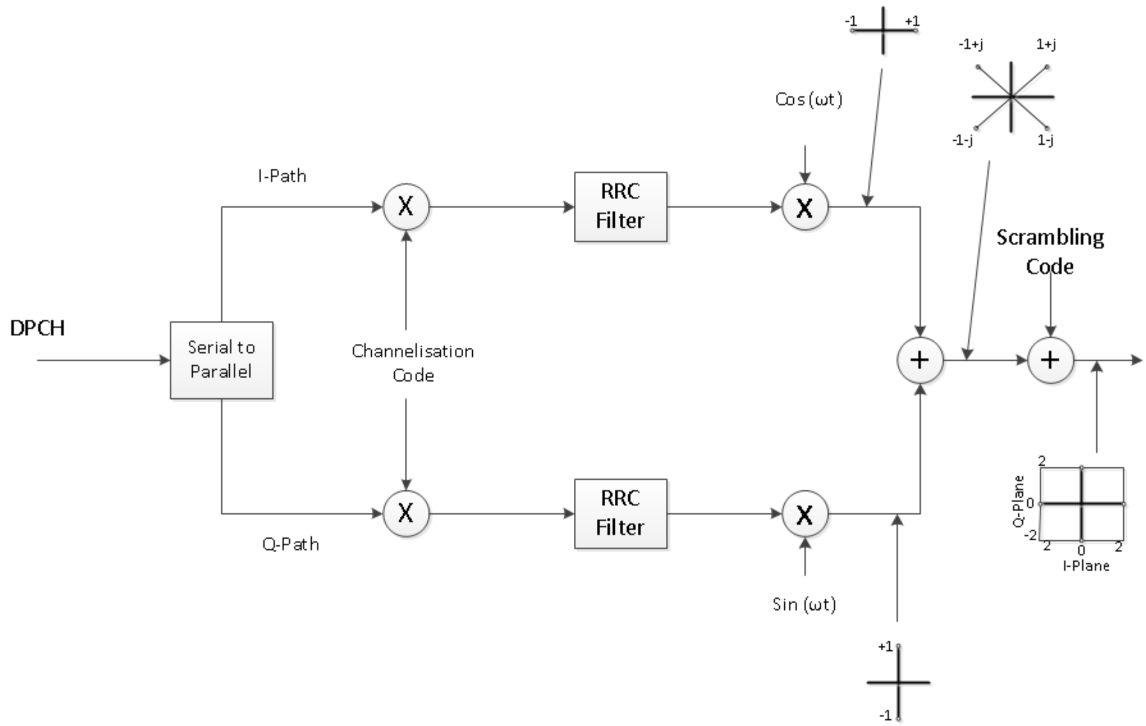

Figure 5.8 Single User Spreading and Scrambling Operation [5]

QPSK relies on phase variation of the signal. The phase of the in-phase stream varies from $0^{\circ}\ to\ 180^{\circ}$ while that of the quadrature phase stream varies from $90^{\circ}\ to\ -90^{\circ}$. The combination of the two stream leads to a signal which has points at four different phase values as shown in table 5.2. The signal constellation for QPSK signals is shown in figure 5.9.

Table 5.2 QPSK constellation points

Constellation Points	***Phase angle***
$(+\mathbf{1}+\mathbf{1}\boldsymbol{j})$	45°
$(-\mathbf{1}+\mathbf{1}\boldsymbol{j})$	135°
$(-\mathbf{1}-\mathbf{1}\boldsymbol{j})$	-45°
$(+\mathbf{1}-\mathbf{1}\boldsymbol{j})$	-135°

The modulated signal is then multiplied by the complex scrambling code. The multiplication by the scrambling code changes the value of the constellation points to real values in the range of +2, 0 and -2 as shown in figure 5.10.

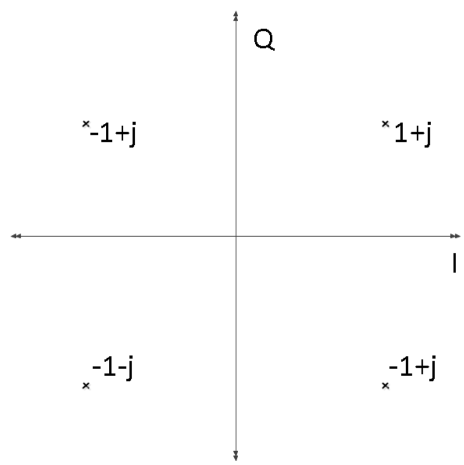

Figure 5.9 Signal Constellation for QPSK signals.

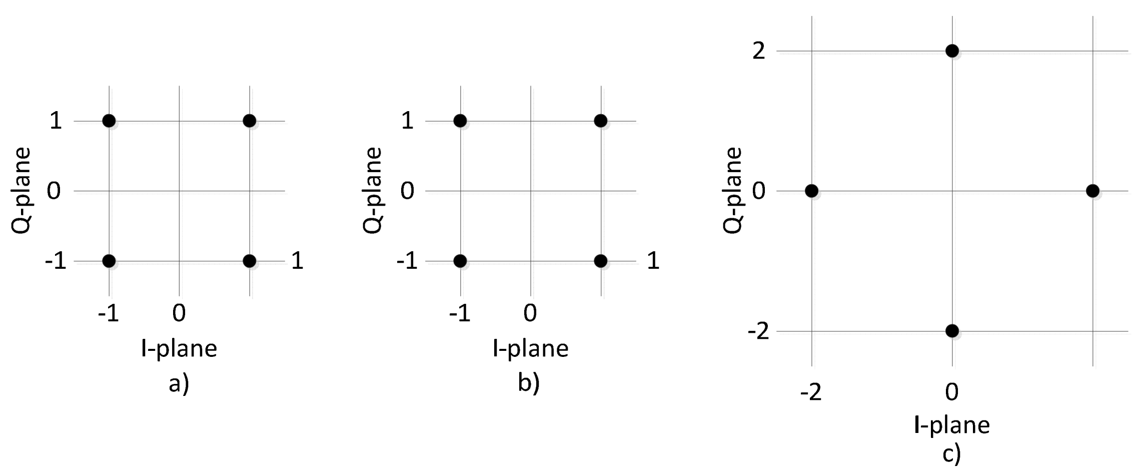

Figure 5.10 Downlink spread constellation a) spread signal phase diagram b) scrambling code spread diagram c) phase diagram after spreading and scrambling [5]

5.4.1 Multiple Users

Now consider the case, when multiple users are present in the system. In this case, streams from each of the two users are passed through a serial to parallel component to form In-phase (I) and Quadrature phase (Q) streams. For each user, the I-plane and Q-plane streams are first multiplied with the user specific channelisation code. Then each of the I-plane chip streams from different users are added to form a combined I-plane chip stream, and a similar combination takes place for the Q-plane chip streams. The combined I-plane chip stream is multiplied by an RF carrier (cosine waveform) and the combined Q-plane chip stream is multiplied by a 90° phase shifted RF carrier (sine waveform). These two streams are then added to form the QPSK symbols. The modulated output is then multiplied with the complex scrambling code. Figure 5.11 illustrates the above operation, when two different users are present in the system.

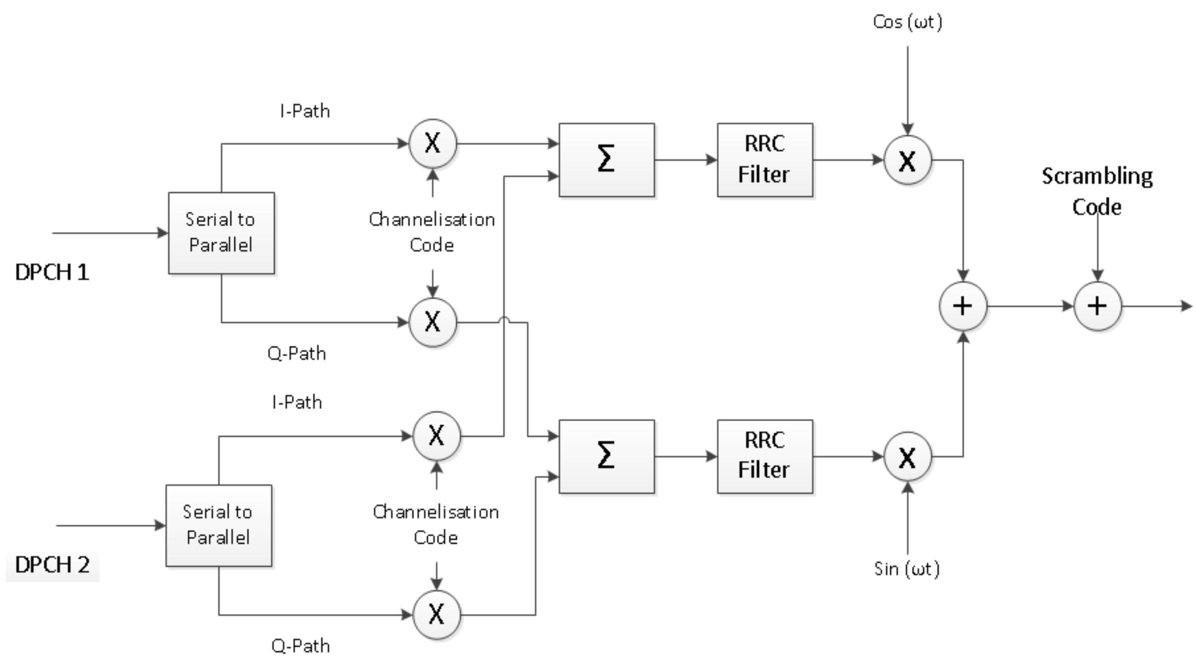

Figure 5.11 Spreading and scrambling operation for Multiple Users [5]

The amplitude of each of the user signals is different in real world, since this value depends upon the distance of the user from the Node B. The users far away from the Node B would need more power, while those closer require less power. Also the signal power is also dependent on the data rate required for the user. For simulation purposes, we have considered each of the user signals with unity gain. The scrambled output for two and four equal power users is shown in Figure 5.12.

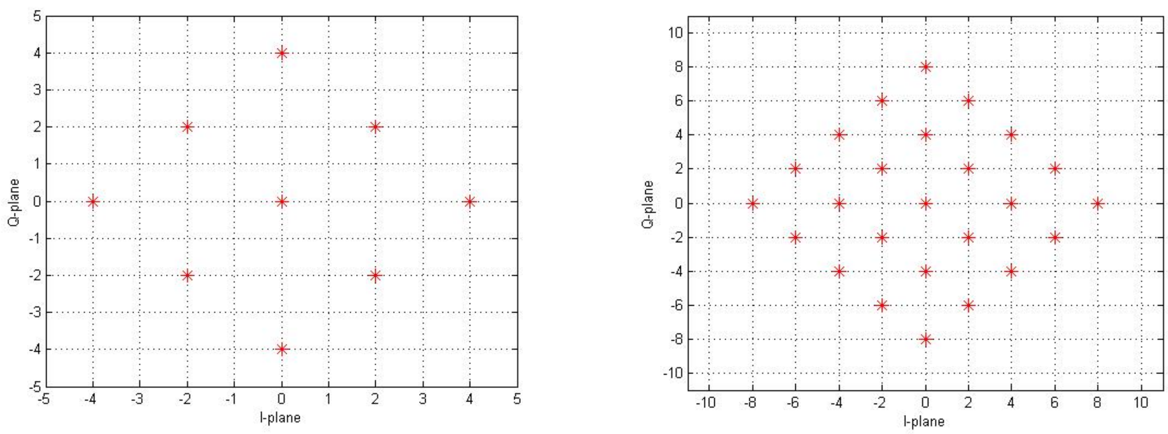

a) b)

Figure 5.12 Scrambled output for a) 2 users b) 4 users [5]

5.5 Upsampling

After scrambling, up sampling of the data is carried out. Up-sampling introduces a set of zeros between consecutive chips depending on the up-sampling factor. In our simulation, we have used an up sampling factor of eight; hence seven zeros are inserted between consecutive chips. The up-sampler converts the chips into samples, and thus, the data rate is now defined by the sampling rate. Up sampling, along with pulse shaping filter helps in reducing the error, due to improper synchronization at the receiver.

5.6 Pulse Shaping Filter

The output of the up-sampler is given to a pulse shaping filter. The QPSK modulation used in the WCDMA system, results in adjacent channel sidebands, which may cause interference to adjacent frequencies used by some other users. To prevent this interference, some form of filtering is required at the transmission side. This filtering is done by using a pulse shaping filter. The most commonly used pulse shaping filter is the raised cosine filter. The raised cosine filters are examples of Nyquist filters providing almost zero inter-symbol interference at the optimum sampling point of filtered data. {{14 Richardson,Andrew 2005; }}

The transfer function of the raised cosine filter in the frequency domain is given by

$$H(f) = \begin{cases} T & 0 \leq |f| \leq \dfrac{1-\alpha}{2T} \\ T/2(1+\cos[\dfrac{\pi T}{\alpha}(|f| - \dfrac{1-\alpha}{2T})]) & \dfrac{1-\alpha}{2T} \leq |f| \leq \dfrac{1+\alpha}{2T} \\ 0 & |f| > \dfrac{1+\alpha}{2T} \end{cases}$$

The parameter 'α' in the above equations is known as the roll-off factor and defines the frequency response of the raised cosine filter. The value of 'α' is chosen to be 0.22 for the WCDMA system. Figure 5.13 shows the time domain response of a raised cosine filter with sampling factor of eight and value of $\alpha = 0.22$.

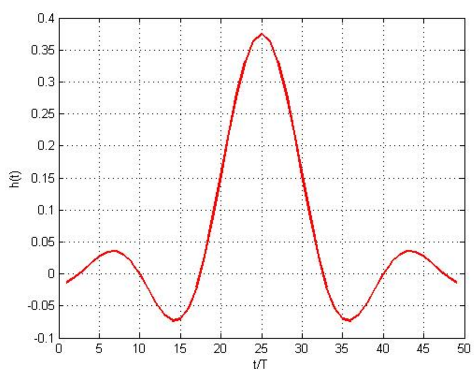

Figure 5.13 Time domain response of raised cosine filter

The output of the pulse shaping filter is then transmitted through the channel to the user terminal using the radio equipment present at Node B.

CHAPTER 6

CHANNEL AND NOISE SIMULATION

Mobile radio propagation results into two types of fading – large scale fading and small scale fading. Large-scale fading represents the average power attenuation or path loss of the signal when the user moves over large areas inside the cell.[10]. Small scale fading represents the time spreading of the signal due to relative motion over short distances and the time variant behavior of the channel. The different types of fading can be classified into different types as shown in figure 6.1. The details of these classifications are given in [10].

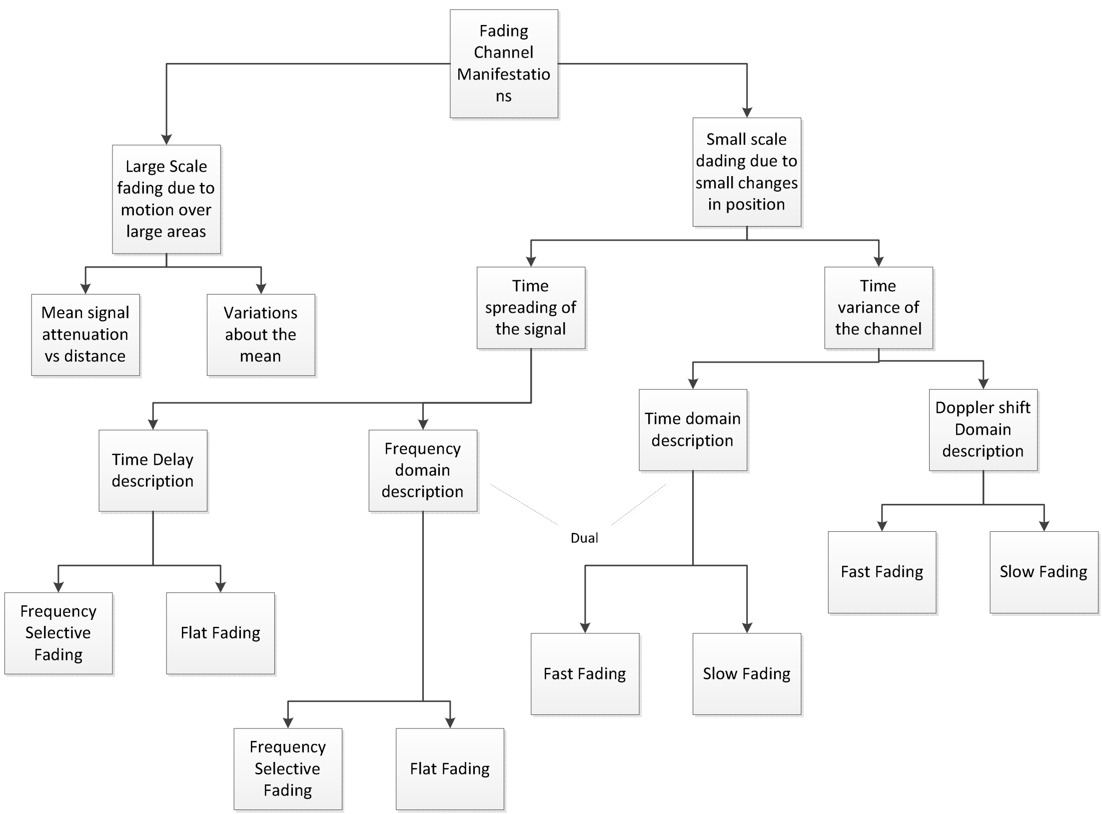

Figure 6.1 Types of fading [10]

6.1 Small Scale Multipath Fading

At distances in order of wavelengths, there is large variation of the signal level especially when the receiver is moving. This is known as small scale fading. Small scale fading is attributed to the following factors:[8]

Multipath propagation: The transmitted radio wave propagates via reflection, scattering and diffraction through the air interface between the Node B and user terminal due to various obstacles present in its propagation path. This gives rise to multiple delayed versions of the same signal and is known as multipath propagation. Due to multipath propagation, the delayed versions of the signals can have large propagation delays leading to inter-symbol interference.

Speed of the Mobile: The frequency of the signal gets shifted due to motion between the user equipment and Node B. The rate of change is directly proportional to the velocity of the user. This shift in frequency is known as Doppler shift. Depending on the direction of the user from the Node B, Doppler shifts can be positive or negative.

Speed of the surrounding objects: If the objects in the transmission path like vehicles are also in motion, then this relative motion also causes Doppler shift in the frequency of the multipath components. This effect is taken into consideration only if the objects are moving faster than the user.

Transmission bandwidth of Channel: The received signal is distorted if the bandwidth of the transmitted signal is greater than the coherence bandwidth of the channel.

For macro cellular systems with large cells this signal variation is characterized by a Rayleigh distribution while for microcellular systems where a direct line of sight is available these signal variations are characterized by a Ricean distribution [9]. A mobile radio roaming over a large area must process signals that experience both types of fading: small-scale fading superimposed on large-scale fading [10].

6.2 Flat and Frequency Selective Fading

Flat Fading: In time domain, if the maximum path delay is less than the symbol time, then the channel is said to be flat fading or frequency non-selective fading channel. In this case, all the delayed components of the signal arrive within the symbol time, and hence, there is no inter-symbol interference. However, there is still fading due to the destructive interference between the multipath components.

In frequency domain, the channel is said to exhibit flat fading, if the coherence bandwidth is greater than the signal bandwidth. The coherence bandwidth is defined as that bandwidth of the channel through which the signal passes experiencing approximately equal gain and linear phase. Hence, all the frequency components present in the signal will undergo identical amount of fading [10].

Frequency Selective Fading: In time domain, if the maximum path delay of the multipath components is greater than the symbol time, then the channel is said to be frequency selective fading channel. Hence, some of the multipath components arrive during the next symbol duration causing inter-symbol interference. This distortion can be reduced since the multipath components can be resolved at the receiver using a rake receiver.

In the frequency domain, the channel is said to be frequency selective, if the coherence bandwidth of the channel is less than the signal bandwidth. The name is derived from the fact that all the spectral elements of the signal are affected differently by the channel.

6.3 Rayleigh Flat Fading Channel

For non line of sight signal propagation through the air interface, the channel fading is characterized by Rayleigh distribution. The simulation for the Rayleigh fading channel is in general, carried out using Jake's model by sum of sinusoids method. This method assumes that the entire multipath has equal strength, and the channel is non frequency selective. Consider a baseband signal $s(t)$ given by

$$s(t) = re\{\tilde{s}(t)e^{j2\pi fct}\}$$

If the channel is comprised of 'N' propagation paths, then the received waveform is given by

$$r(t) = Re[\sum_{n=1}^{N} C_n e^{j2\pi[(fc+fdn)(t-\tau_n)]}\tilde{s}(t-\tau_n)$$

Where $r(t) = s(t) * g(t,\tau)$

$g(t,\tau)$ Is the channel response

C_n Is the amplitude gain

τ_n Is the time delay, associated with nth propagation path

$f_{d,n}$ Is the Doppler shift for path 'n'.

After complex mathematical manipulations [11], the channel response reduces to

$$g(t) = \sum_{n=1}^{N} e^{j(2\pi fmtcos\theta n+\emptyset_n)}$$

This can be rewritten in terms of in-phase and quadrature phase components as

$$g(t) = g_I(t) + g_Q(t)$$

Where $$g_I(t) = \sum_{n=1}^{M} 2cos\beta_n cos\,\omega_n t + \sqrt{2}cos\omega_m tcos\alpha$$

$$g_Q(t) = \sum_{n=1}^{M} 2sin\beta_n cos\,\omega_n t + \sqrt{2}cos\omega_m tcos\alpha$$

The parameters contained in the above equations are

$N = Number\ of\ multipath\ components\ (\geq 60)$

$\omega_m = 2\pi f_m is\ the\ maximum\ Doppler\ shift$

$\omega_n = \omega_m \cos\left(\frac{2\pi n}{N}\right) is\ the\ Doppler\ shift$

$M = \frac{1}{2} * \left(\frac{N}{2} - 1\right) are\ the\ low\ frequency\ oscillators\ needed\ to\ generate\ the\ sinusoids$

$\beta_n = \frac{n\pi}{M} and\ \alpha = 0$

The channel gain is normalized so that its maximum value is unity. The normalized values are given by

$$g'_I(t) = \frac{g_I(t)}{\sqrt{M+1}}$$

$$g'_Q(t) = \frac{g_Q(t)}{\sqrt{M}}$$

The final Rayleigh channel co-efficient is given by

$$g'(t) = g_I'(t) + g_Q'(t)$$

6.4 Ricean Flat Fading

If a line of sight propagation path is present between Node B and the user equipment in addition to multipath, the fading is characterized by Ricean fading.

Figure 6.2 illustrates how ricean channel co-efficients are generated in simulation using Rayleigh channel co-efficients and parameters A and B.

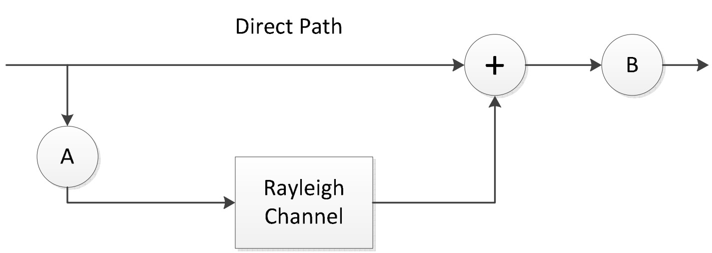

Figure 6.2 Simulation of Ricean Channel [1, 2]

The main parameters defining ricean fading are listed below

$fd = Doppler\ Shift$

$K = Ricean\ Fading\ factor\ (defined\ in\ dB)$

$$K(db) = \frac{direct\ path\ power}{scatterred\ path\ power} = \frac{1}{A^2}$$

$B = Normalizing\ factor\ for\ the\ channel = 1/\sqrt{1 + 10^{-K/10}}$

6.5 Frequency Selective Rayleigh Channel

The bandwidth of WCDMA systems is generally, greater than the coherence bandwidth of the channel, hence frequency selective Rayleigh fading is the most likely scenario in the air interface of a UMTS system. The channel co-efficients can be generated by using a FIR (Finite Impulse Response) filter, whose tap weights are time varying Rayleigh channel co-efficients.

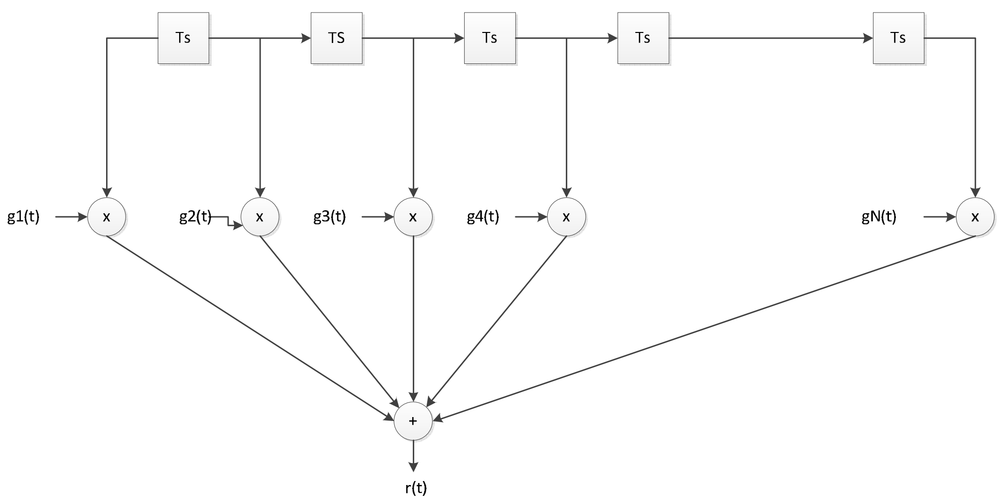

Figure 6.3 Frequency Selective Rayleigh Fading Channel filter structure

In the matlab simulation, four multipath frequency selective Rayleigh fading channel is simulated. The delays of the multipath are taken to be one chip interval. The magnitudes of the multipath components are 0, -3, -6 and -9 db respectively. The Doppler shift fd is taken to be 200 Hz. Figure 6.4 shows an example of the simulated channel.

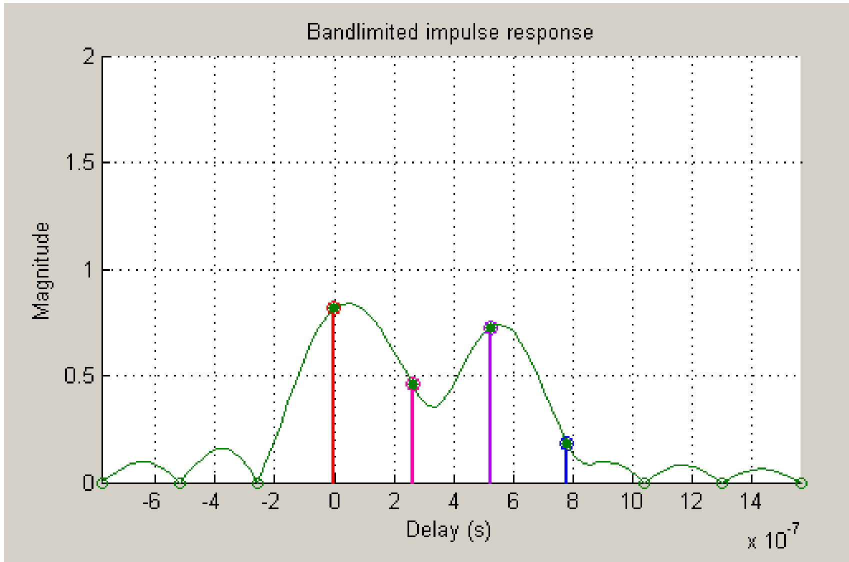

a)

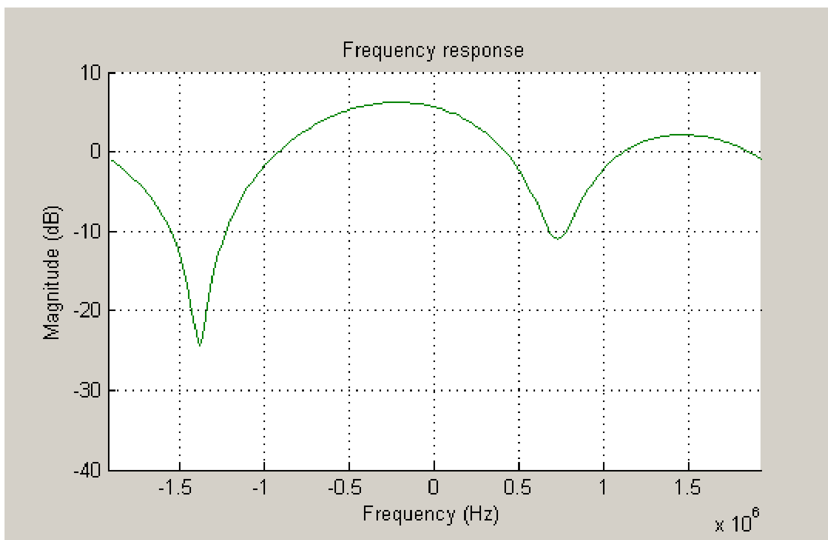

b)

Figure 6.4 Frequency selective Rayleigh channel a) Impulse response b) Frequency response

6.6 Additive White Gaussian Noise (AWGN)

Noise is a form of random signal arising from natural sources. The most common form of noise is additive white Gaussian noise. The term additive means that the noise is added to the signal, and it is statistically independent of the signal, while the term white means that the power spectral density of the noise signal is flat across the whole spectrum.

The amount of noise to be added depends on the signal to noise ratio (SNR) of the system. SNR is generally calculated using the bit energy (Eb), Noise Power (No) and also depends on the modulation scheme used.

$$SNR = \frac{Eb}{No} + log_{10}(k)$$

Where k is the bits/symbol

For QPSK modulation, two bits are used to generate a symbol. Therefore k=2

$$SNR = \frac{Eb}{No} + log_{10}(2) = \frac{Eb}{No} + 3$$

Also from the general definition of signal to noise ratio

$$SNR = 10log_{10}(\frac{signal\ power}{noise\ power})$$

Where signal power is equal to the variance of the signal.

Hence the noise power is given by

$$Noise\ power = \frac{signal\ power}{10^{SNR/10}}$$

For generating complex AWGN noise, two random streams of data are generated in matlab and multiplied by the noise power separately and then added together.

The received signal at the receiver is given by

$$r(t) = h(t) * s(t) + n(t)$$

Where $s(t)$ is the transmitted signal

$h(t)$ is the channel response

$n(t)$ is the AWGN noise

Figure 6.5 shows the channel model with the fading block and additive white Gaussian noise block. Both these blocks are implemented by different functions in Matlab.

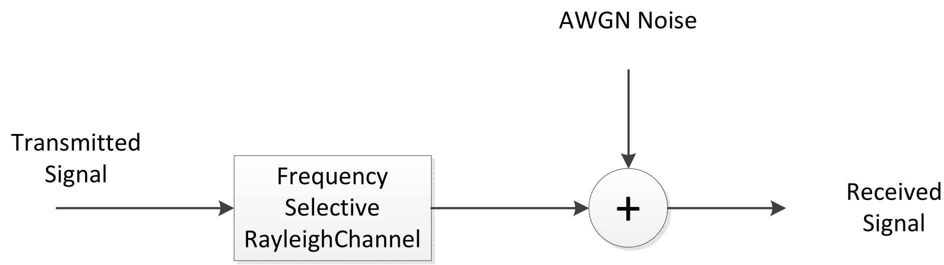

Figure 6.5 Channel Block Diagram [1, 2]

CHAPTER 7

PHYSICAL LAYER SIMULATION OF RECEIVER

7.1 Signal Processing Block

The signal after reception is given to the signal processing block, which is located at the front end of the receiver. Since SPB is used for reduction of the noise before the actual demodulation of the signal takes place, it is located at the front end of the receiver. The SPB consists of the following blocks:

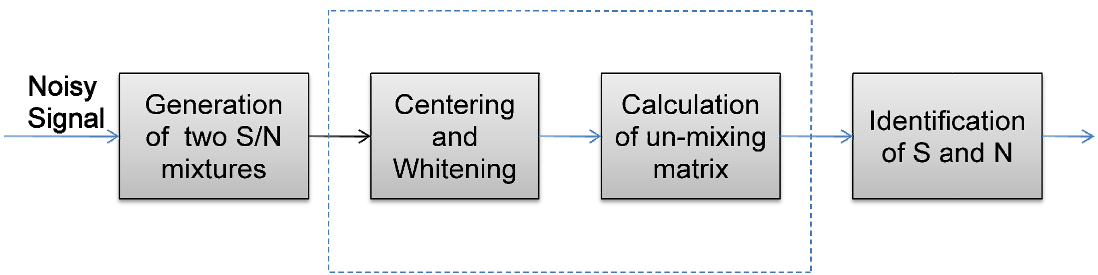

Figure 7.1 Block diagram of signal processing block (SPB) [1]

7.1.1 Generation of two signal and noise mixtures

ICA requires that there must be at least as many different signal mixtures available as the number of source signals. For our case, there is only one mixture available at the receiver end. To solve this problem, a second mixture was generated by adding more noise to the existing mixture, using a similar noise model [2]. Now the two mixtures can be represented in matrix form as , where is a column matrix containing the two mixtures, is the mixing can matrix and, is a column matrix containing the set of original signals. The above matrix equation be rewritten as To obtain the original source signals from the two mixtures; we need to find the un-mixing matrix given by .

7.1.2 Centering

Centering is a pre-processing step used to simplify the ICA process. The mean vector 'm' of the matrix X is first calculated, and then subtracted from X. This will effectively convert X into a zero mean matrix. Once the mixing matrix A is estimated, the mean vector of S given by $A^{-1}m$ can be calculated, and added back to S to complete the estimation process [12].

7.1.3 Whitening

Whitening is an additional pre processing step that is used to transform the vector X linearly into a vector $\widetilde{X}$, whose elements are uncorrelated to each other, and have unity variances. The covariance matrix of such a vector is equal to the identity matrix.

$$E\big(X\,\widetilde{X}\big) = I$$

Whitening is carried out through eigenvalue decomposition (EVD) of the covariance matrix

Using EVD, the covariance matrix is given by the following equation

$$E(XX^T) = EDE^T$$

Where $E\ is\ the\ orthogonal\ matrix\ of\ eigenvectors\ of\ E(XX^T)$

$D\ is\ the\ diagonal\ matrix\ of\ the\ eigen\ values$

For the vector $\widetilde{X}$, the following transformation is used

$$\widetilde{X} = ED^{1/2}E^TX$$

However, we know that $X = AS$

Therefore, $\widetilde{X} = ED^{1/2}E^TAS$

$$\widetilde{X} = \tilde{A}S$$

Now $E(XX^T) = \tilde{A}E\{SS^T\}\tilde{A}^T = \tilde{A}\tilde{A}^T = I$

Thus, whitening converts the mixing matrix A into an orthogonal matrix. The orthogonal matrix has a greater degree of freedom, and hence, fewer elements need to be estimated, reducing the complexity of the overall process.

7.1.4 Calculation of un-mixing matrix

The un-mixing matrix is estimated by using the gradient ascent rule defined in [1, 2]. The gradient ascent rule is defined as

$$W_{new} = W_{old} + l[I - f(U)U^T]W_{old}$$

Where initially the un-mixing matrix W is taken to be an identity matrix, and then a set of iterations is carried out according to the above equation to calculate W.

In the above equation , $U = WX$, where X is the vector containing the two mixtures after centering and whitening, l is the learning rate defined here to be 0.0001, which can be changed to optimize the system, and $f(u) = \frac{1}{1+e^{-u}}$.

Using the estimated un-mixing matrix, we can now find the source vector S which contains the reasonably noise free signal and the noise [2].

7.1.5 Identification of Signal and Noise

The identification of the signal is done by using the autocorrelation property. The autocorrelation for the additive white Gaussian noise is given by $R_{XX}(n, n+m) = \sigma^2\delta(m)$.

The information signal on the other hand, would have a wide autocorrelation value about the mean 'm' due to up-sampling and linear interpolation carried out at the transmitter. This will help in distinguishing the information signal from the noise.

7.2 Matched Filter and Down-sampling

The matched filter is identical to the pulse shaping filter, present in the transmitter. The matched filter is implemented to reject the noise and interference present in the received signal. If the transfer functions of the pulse shaping filter is $H_T(f)$ and that of the matched filter is $H_R(f)$, then the combined transfer function of the system is given by

$H_{SYS}(f) = H_T(f)\, H_R(f)$

If the same filter is used in both the cases; this is what is meant by the name matched filter, the combined transfer function is

$H_{SYS}(f) = |H_T(f)|^2$

Hence, $sqrt[H_{sys}(f)] = sqrt\ (RC)$

Where RC is raised cosine

Therefore, both the transmit and receive side use root of raised cosine filter.

Similar to the up-sampling operation in the transmitter, down sampling takes place in the receiver. Down-sampling implies choosing a single sample from the available eight samples. Down-sampling converts the data rate from samples/sec to chips/sec.

7.3 Rake Receiver

The rake receiver is implemented in the WCDMA receiver, in order to receive, descramble, de-spread and combine the different multipath components together. The combining in rake receiver can be carried out in two ways: chip level combining and symbol level combing. In symbol level combining, data is first descrambled and de-spread, before multipath combination takes place. In chip level combining, the signal is first multiplied by the conjugate of the channel co-efficients, and then descrambling and dispreading take place. We have implemented a symbol level combining rake receiver to avoid the complexity in the system.

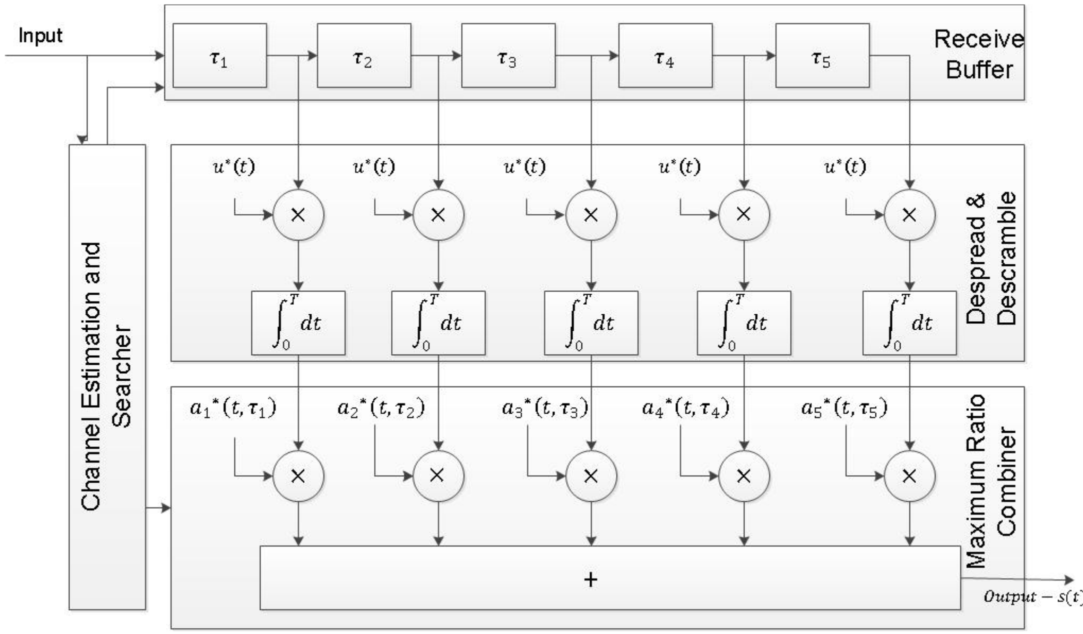

Figure 7.2 Rake receiver structure [5]

The following steps occur in a WCDMA rake receiver:

- Descrambling: The delays for the multipath signals are first found by using a path searcher. Each delay corresponds to a separate multipath that is to be combined using the rake receiver. At each of the rake branches, the received signal is delayed by some amount as determined by the path searcher, and is then multiplied by the conjugate of the scrambling code.

- De-spreading: The descrambled data of each path is de-spread by simply multiplying the descrambled data by the user specific channelisation code. This channelisation code is the same as the one used at the transmitter.

- Integration and dump. The de-spread data is integrated over one symbol period, giving one complex output per QPSK symbol. This process is carried out for all paths to be combined by the rake receiver.

- Channel equalization: Each of the multipath signals is then multiplied with the conjugate of the estimated channel co-effcients. The channel estimates can be obtained from the CPICH channel or/and the pilot bits contained in the DPCCH.

- Symbol combining: The same symbols obtained via different paths are then combined using maximal ratio combining (MRC).

- Demodulation: The combined output is sent to a simple decision device to demodulate the QPSK symbols.

CHAPTER 8

HIGH SPEED DOWNLINK PACKET ACCESS SYSTEM (HSDPA)

8.1 Introduction

High Speed Downlink Packet Access (HSDPA) system is an upgrade to the existing 3G networks providing clear capacity improvements and higher data rates. The main characteristics of an HSDPA system are listed below:

8.1.1 HS-DSCH or High Speed Downlink Shared channel

The High Speed Downlink Shared Channel is a downlink transport channel shared by several UEs. HS-DSCH can have a peak data rate of up to 10 Mbps, when 16 quadrature amplitude modulation (QAM) is used in the physical layer. The transmission time interval (TTI) has been shortened to 2 ms as compared to earlier systems. The shorter frame duration leads to faster transmission and retransmission. The spreading factor for HS-DSCH is fixed at 16. HS-DSCH can use both QPSK modulation and 16 QAM [23].

HS-DSCH is always used in conjunction with High speed Shared Control Channel (HS-SCCH). The HS-SCCH carries all information required by the user to decode the information on HS-DSCH. The HS-SCCH frame with three slots can be divided into two logical parts. The first part consisting of one slot gives information about the channelisation code and the modulation used on HS-DSCH. The second part gives information about the ARQ (automatic repeat request) process, retransmission status etc [6].

8.1.2 Adaptive Modulation and Coding (AMC)

HSPDA standard ensures that highest possible data rate is achieved for all users regardless of whether they are close to the base station or far by choosing the transport format, including the modulation scheme and code rate based on the downlink channel. For example consider a downlink scenario, where the user is close to the Node B and, it is not possible for the Node B to reduce the power through power control. In HSDPA, this problem is solved by choosing a modulation and coding scheme which has a higher requirement of SNR, thus effectively making the UE use the additional power from Node B [22].

8.1.3 Hybrid Automatic Repeat Request (HARQ)

HARQ is a link adaptation scheme, which is used by the system to provide faster retransmissions through link layer acknowledgements. In case of ARQ (automatic repeat request), if CRC check fails then the packet is discarded, but in HARQ the packet is stored and in case the re-transmitted packet is again erroneous then the previous and current packet is combined in an attempt to recover from errors. For earlier 3G systems, the retransmissions originated from the serving RNC leading to large delay. With HSDPA systems, medium access control (MAC) layer is present at the Node B and, hence retransmissions can take place from Node B itself leading to shorter delays [6].

8.2 Physical layer simulation of a HSDPA system

Figure 8.1 shows the physical level block diagram for a HS-DSCH frame. Most of the blocks are common to that used by DCH in the UMTS system. The blocks which are significantly different are explained below:

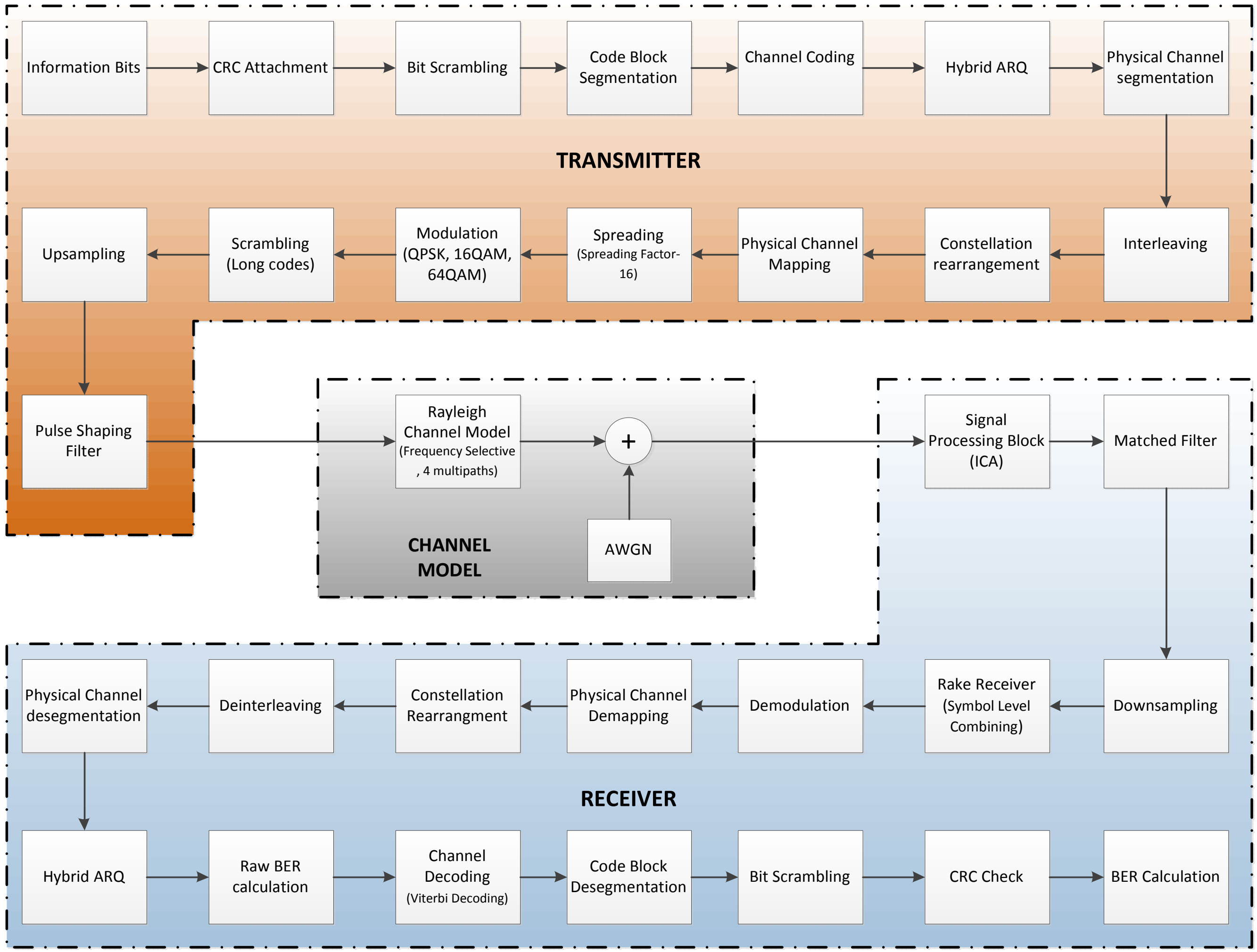

Figure 8.1 Physical layer block diagram of a 3G HSDPA system with SPB

8.2.1 Bit Scrambling

The bits obtained after CRC attachment were scrambled according to the following algorithm:[13]

- Consider the bits input to the bit scrambler are given by $b_1, b_{2,} b_3 \dots \dots b_B$, where B is the total number of bits. Let the bits after descrambling be given as $d_1, d_{2,} d_3 \dots \dots d_B$.
- The equation below is used to scramble the bits

$$d_i = (b_i + y_k) mod2 \qquad\qquad where\ k = 1,2..B$$

$y_k\ in\ the\ above\ equation\ is\ calculated\ below$

$$y'_\gamma = 0 \qquad -15 < y < 1$$

$$y'_\gamma = 1 \qquad y = 1$$

$$y'_\gamma = \left(\sum_{x=1}^{16} g_x\, y'_{\gamma-x)}\right) mod2 \qquad 1 < y < B$$

Where $g = \{g_1, g_2, g_3 \dots \dots \dots \dots \dots \dots g_{16}\} = \{0, 0, 0, 0, 0, 0, 0,0, 0, 0, 1, 0, 1, 1, 0, 1\}$

$$y_k = y'_k \qquad k = 1,2 \dots B$$

8.2.2 Hybrid ARQ (HARQ)

The HARQ block uses a two stage rate matching as shown in figure 8.2. The buffer between the rate matching stages can be used to change the settings for the retransmission process. The HARQ can be done in two different ways. In the first type, identical retransmissions are sent, once the CRC check fails. This is known as chase or soft combining. In the second type, the first transmission can contain systematic bits while the latter one can contain parity bits [6].

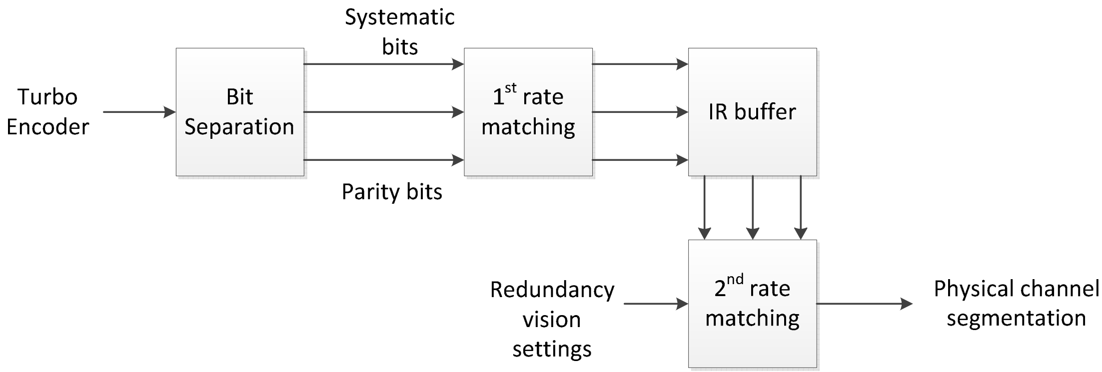

Figure 8.2 HARQ function principle [6]

8.2.3 Interleaving and Constellation rearrangement

The interleaving operation is similar to that carried out by the second interleaver in UMTS. There are three interleaver blocks present as shown in figure 8.3. For QPSK modulation, only the first interleaver is used. For 16 QAM, the first two interleaver blocks are used with first two bits going to the first one and the next two to the second one. For 64 QAM, all three interleaver blocks are used with two bits going to each interleaver.

Constellation rearrangement is used to change the positions of the bits mapping to the modulated symbols. It is only valid for 16 QAM and 64 QAM.

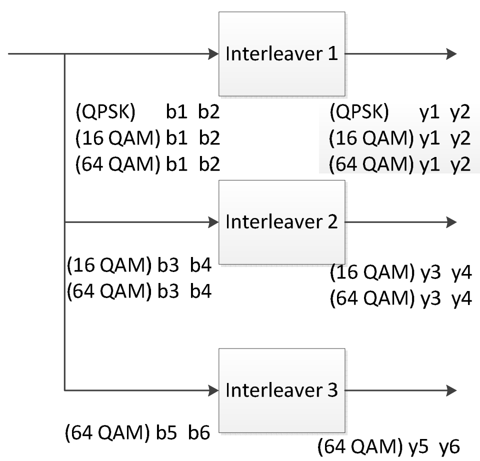

Figure 8.3 Interleaver structure for HS-DSCH [14]

CHAPTER 9

PERFORMANCE ANALYSIS AND SIMULATION RESULTS

9.1 Performance Analysis

The physical layer of a 3G UMTS and HSDPA systems were simulated in Matlab. Performance analysis was carried out by measuring the bit error rate (BER) and frame error rate (FER).

$$Bit\ error\ rate\ (BER) = \frac{number\ of\ bits\ in\ errorr}{total\ number\ of\ bits\ transmitted}$$

$$Frame\ error\ rate\ (BER) = \frac{number\ of\ frames\ in\ errorr}{total\ number\ of\ frames\ transmitted}$$

The simulation is carried out for a thousand different frames under varying channel conditions, and in presence of randomly generated noise. The comparison is carried out by measuring the BER, when the SPB is present in the system, and, when the SPB is removed. The results are plotted on an Eb/No vs BER plot for values of Eb/No ranging from -1 to 8. Further, to extend the importance of the system to data applications, frame error rate calculation is also carried out and a similar comparison made. All simulations are carried out in Matlab R2010a.

The channel used is Rayleigh fading frequency selective channel with four multipath components. Each of the multipath components has a delay equal to one chip interval. The chip rate of the system is defined as 3.84 Mcps and, hence the symbol time turns out to be 2.6042e-007 sec. Additive white Gaussian noise is added in the system after the channel model.

The signal processing block carries out twelve iterations for each sample for the convergence of the gradient ascent equation and the learning rate is set to 0.0001.

9.2 Matlab Simulation

9.2.1 Basic wireless communication system with Rayleigh and Rican fading

The SPB was first tried out, with a basic wireless communication system similar to GSM system. The system was developed by Sudeep Sharma and AbhijeetKumar Singh [1, 2]. The block diagram of this system is shown in figure 9.1.

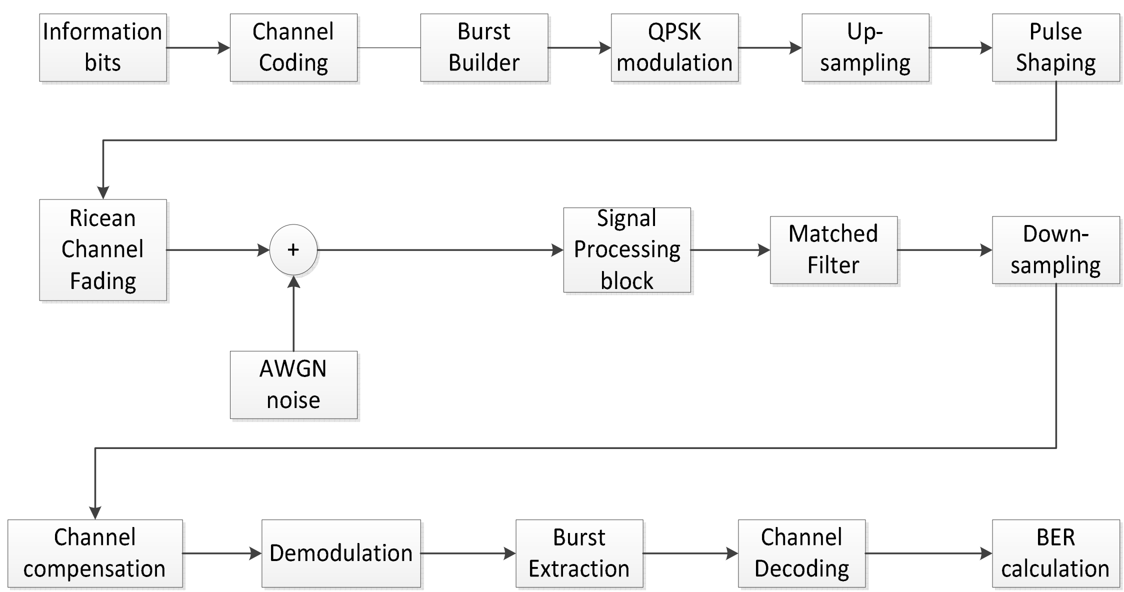

Figure 9.1 Block Diagram of a basic wireless communication system [1]

The transmitter section consists of a ½ rate convolutional encoder, burst builder and a QPSK modulator. The channel is modeled by Ricean distribution, and the noise used is the additive white Gaussian noise. The receiver consists of a channel compensator, which equalizes the channel using linear block phase estimation, and QPSK demodulation using a hard slicer. At the end, BER is calculated between the transmitted and received burst. This simulation is carried out for a thousand frames, and the noise is generated randomly in each case. The results of BER calculation prove that the SPB provides a significant improvement in the system, through reduction of BER, as compared to the system without the SPB in place. The results of this simulation are outlined in the thesis by Sharma [1] and Singh [2].

In this thesis, we performed three different simulations in order to verify the efficacy of SPB in each of them.

I. Basic wireless communication system with Rayleigh flat fading channel

II. 3G UMTS wireless cellular system

III. 3G HSDPA wireless cellular system

The Sharma and Singh system was modified by using Rayleigh flat fading channel, instead of Ricean flat fading. The block diagram of the modified system is shown in figure 9.2. Rayleigh distribution is used to model non line of sight (NLOS) propagation path between the transmitter and the receiver, which is generally the case in macro cellular environment. Ricean distribution is used to model line of sight (LOS) propagation, where a direct visible path is available between the transmitter and the receiver, which is generally the case in micro cellular environment.

The BER calculation was carried out for a thousand different bursts with variation in signal to noise ratio. The results of the calculation are plotted in figure 9.3. From the results, it can be seen, that there is significant reduction in the BER, when the SPB is inserted at the receiver. After proving these results, work started on developing a 3G wireless communication system in order to test the SPB for this system.

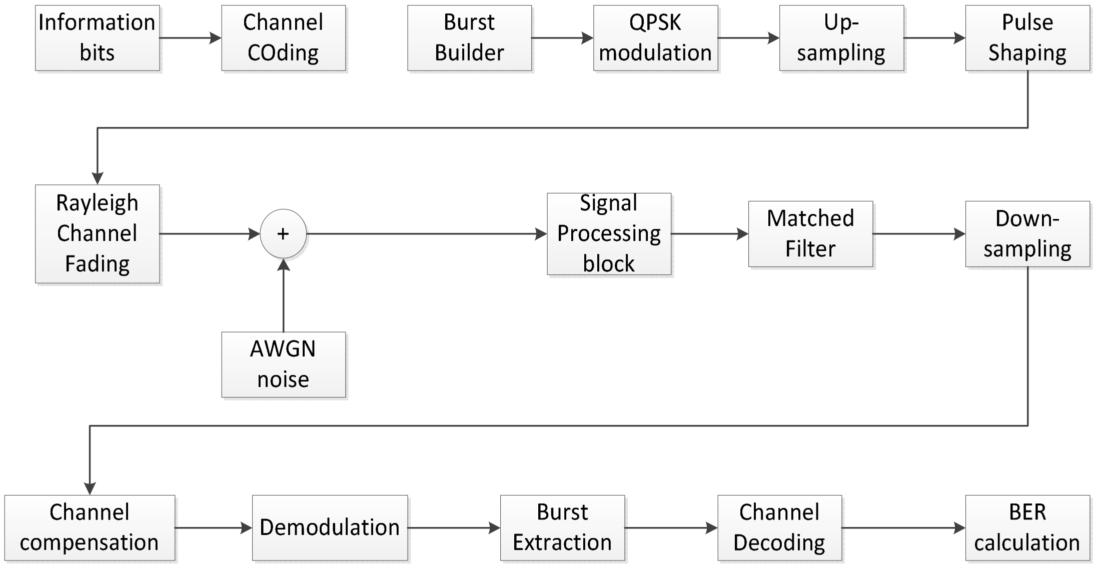

Figure 9.2 Block diagram of the basic wireless communication system with Rayleigh flat fading

9.2.1.1 BER for QPSK modulated signal in basic digital communication system with Rayleigh flat fading channel

Fading	Rayleigh
Doppler Frequency	100 Hz

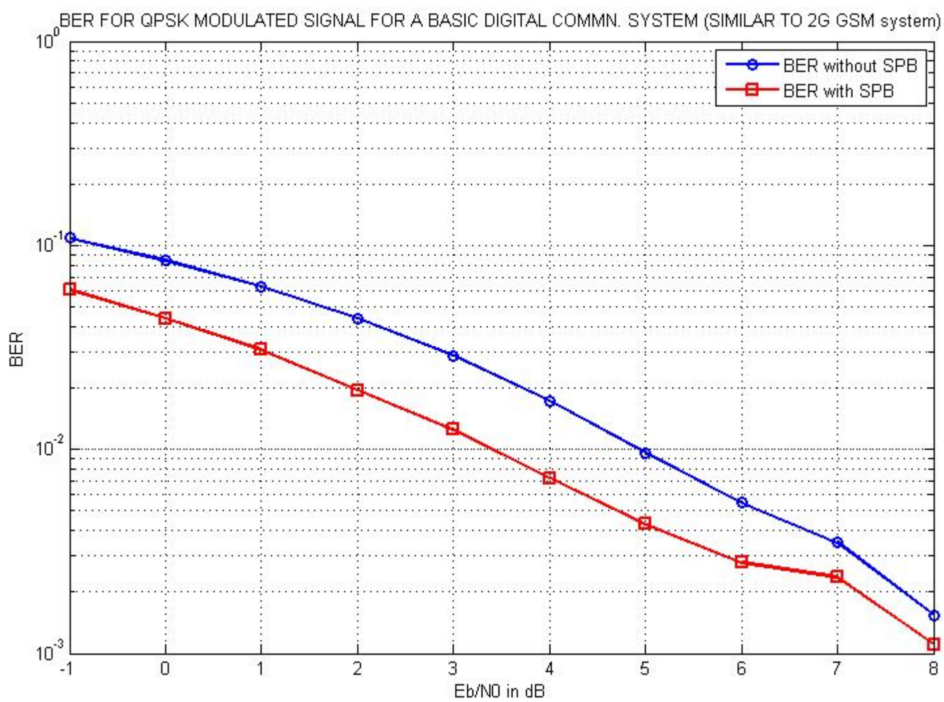

Figure 9.3 BER for QPSK modulated signal in basic digital communication system with Rayleigh flat fading channel.

9.2.2 Simulation of 3G wireless communication system with SPB for single user

The basic block diagram for the physical layer of a 3G wireless communication system is shown in figure 3.2. The transmitter, receiver and channel were implemented in Matlab. The multiplexing scheme used in the system is WCDMA, which is implemented by the spreading and de-spreading function. Due to wideband nature of the transmitted signal spectrum, the channel can no longer be considered to be a flat fading channel, and hence a frequency selective Rayleigh fading channel is simulated. The explanation for the frequency selective channel is given in section 6.5. The rake receiver is used to prevent inter-symbol interference, due to the multipath signals (delayed versions of the transmitted signals arriving in another chip interval) by combining them. The raw bit error rate was calculated at the end, for a thousand different frames with varying channel and noise parameters.

Initially, the simulation was carried out for a single user in the cell. The spreading operation for a single user is shown in figure 5.7. The bit error rate results of the simulation are plotted in figure 9.4. Further, the frame error rate is also calculated, and the simulation results are plotted in figure 9.5.

From the results, we can see that there is significant reduction in the BER values for low values of SNR, when SPB is used in the receiver. As we increase the SNR, the results for BER with the SPB and without it, start to converge. The simulation for FER also presents similar results. Hence, we can conclude that SPB can be used to improve the performance of the system at low SNR values, which happens at the boundaries of the cells. We therefore, believe that SPB will help reduce call drops in existing configurations of the system.

9.2.2.1 BER for QPSK modulated signal in WCDMA based UMTS FDD downlink physical channel with single user

Characteristics	Parameters
Users	1
Channel Type	‘Rayleigh’
Input Sample Period	2.6042e-007
Doppler Spectrum	Jake’s Model
Maximum Doppler Shift	100 Hz
No. of Multipath	4
Path Delays	1.0e-006 * [0 0.2604 0.5208 0.7813]
Avg. Path Gains (dB)	[0 -3 -6 -9]

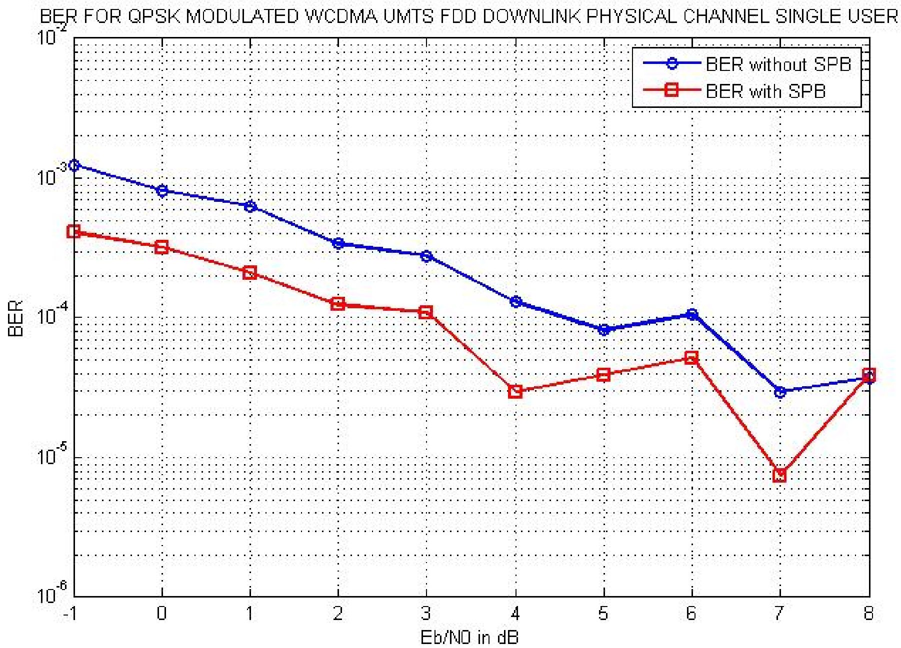

Figure 9.4 BER for QPSK modulated signal in WCDMA based UMTS FDD downlink physical channel with single user.

9.2.2.2 Frame error rate (FER) for QPSK modulated signal in WCDMA based UMTS FDD downlink physical channel with single user

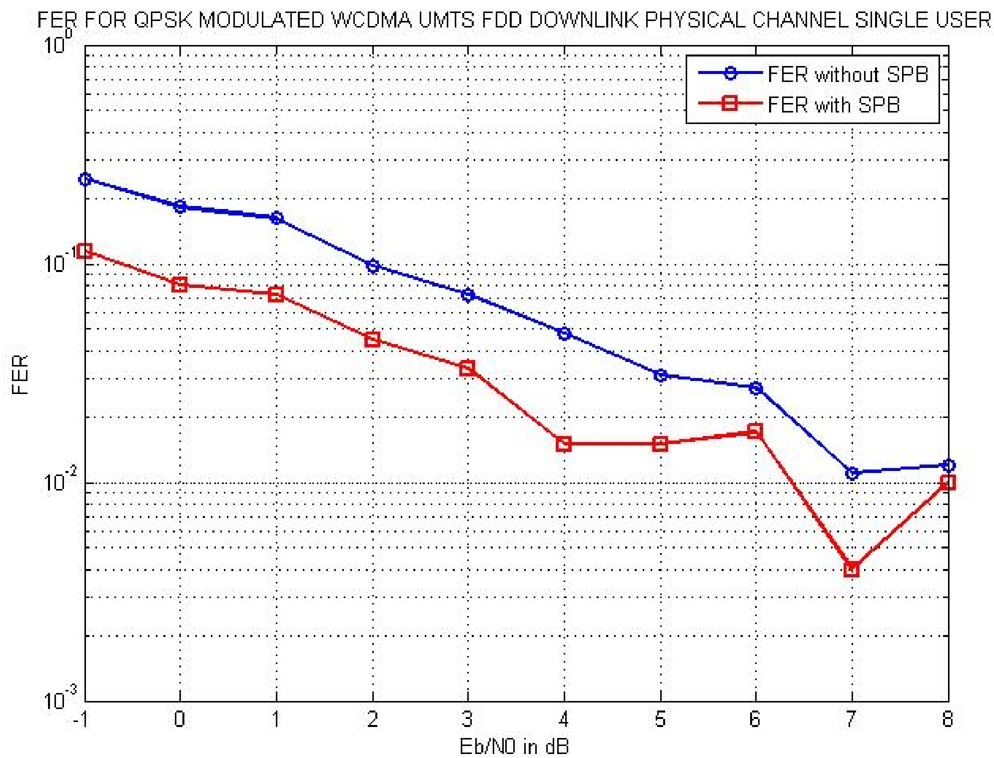

Figure 9.5 Frame error rate (FER) for QPSK modulated signal in WCDMA based UMTS FDD downlink physical channel with single user.

9.2.3 Simulation of 3G wireless communication system with SPB for multiple users

The above simulations were carried out by assuming a single user in the cell. Now consider the real world case, where multiple users are present in the cell. The orthogonality of the channelisation codes is used to separate the desired user information at the receiver. The simulation was first extended to a two user system, and the simulation was carried out with the SPB inserted in the receiver. The spreading and de-spreading operations for two users are shown in figure 5.4. The amplitude of both the users is assumed to be unity. The de-spreading operation at the receiver is carried out through four correlators, to account for the four multipath signals.

The simulation was carried out by transmitting thousand different frames under varying channel and noise parameters, and raw BER was calculated with the SPB in place, and then without the SPB. The results of this simulation are plotted in figure 9.6. The raw FER was also calculated for each of the frames at different SNR values, and the results are plotted in figure 9.7. From the results, it can be concluded that the addition of the SPB to the system causes a significant reduction in the BER and FER at low values of SNR.

The system was further extended for four users. The four users used four different channelisation codes from the OVSF code tree shown in figure 5.1. The receiver uses only the channelisation code of the desired user to decode the information at the rake receiver. The BER and FER results of the simulation for the four user case are shown in figure 9.8 and 9.9 respectively. These results are similar to our earlier results, and prove that the SPB works for different real world scenarios.

9.2.3.1 BER for QPSK modulated signal in WCDMA based UMTS FDD downlink physical channel with two users

Characteristics	Parameters
Users	2
Channel Type	'Rayleigh'
Input Sample Period	2.6042e-007
Doppler Spectrum	Jake's Model
Maximum Doppler Shift	100 Hz
No. of Multipath	4
Path Delays	1.0e-006 * [0 0.2604 0.5208 0.7813]
Avg. Path Gains (dB)	[0 -3 -6 -9]

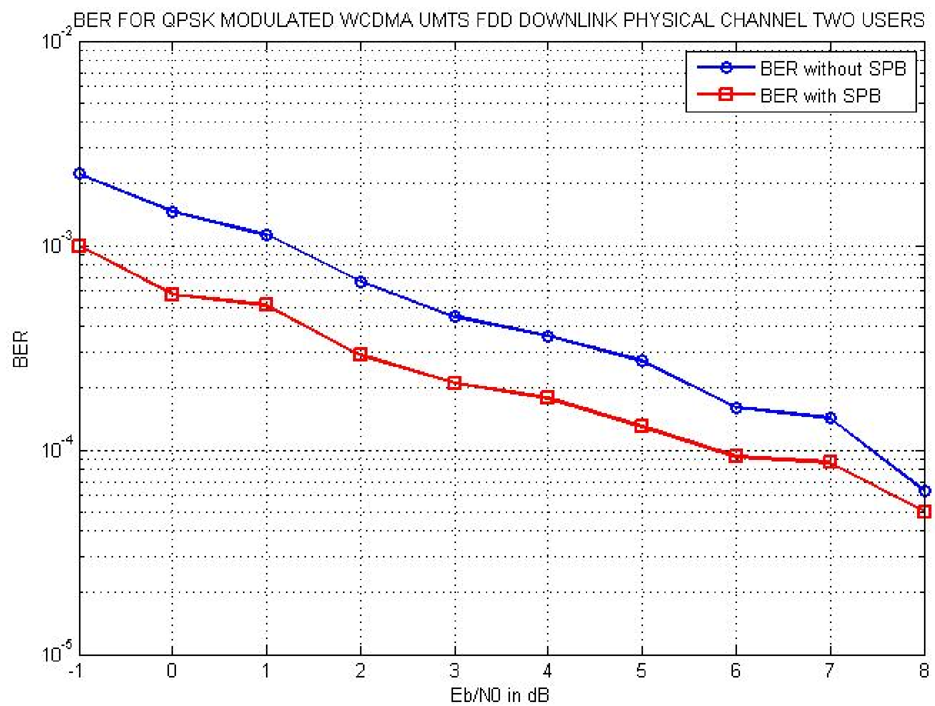

Figure 9.6 BER for QPSK modulated signal in WCDMA based UMTS FDD downlink physical channel with two users.

9.2.3.2 BER for QPSK modulated signal in WCDMA based UMTS FDD downlink physical channel with four users

Characteristics	Parameters
Users	4
Channel Type	‘Rayleigh’
Input Sample Period	2.6042e-007
Doppler Spectrum	Jake’s Model
Maximum Doppler Shift	100 Hz
No. of Multipath	4
Path Delays	1.0e-006 * [0 0.2604 0.5208 0.7813]
Avg. Path Gains (dB)	[0 -3 -6 -9]

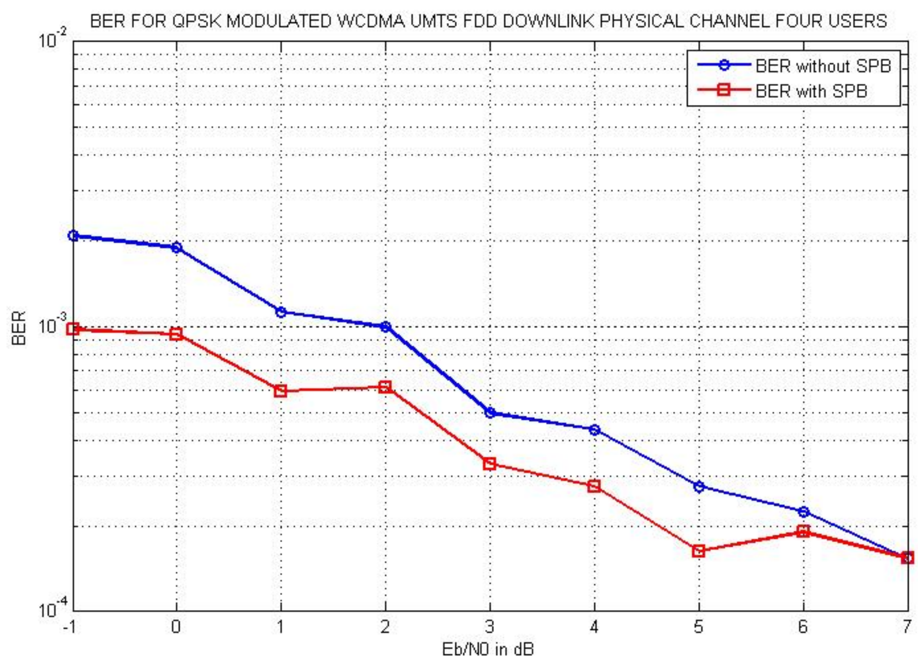

Figure 9.7 BER for QPSK modulated signal in WCDMA based UMTS FDD downlink physical channel with four users.

9.2.3.3 Frame error rate (FER) for QPSK modulated signal in WCDMA based UMTS FDD downlink physical channel with two users

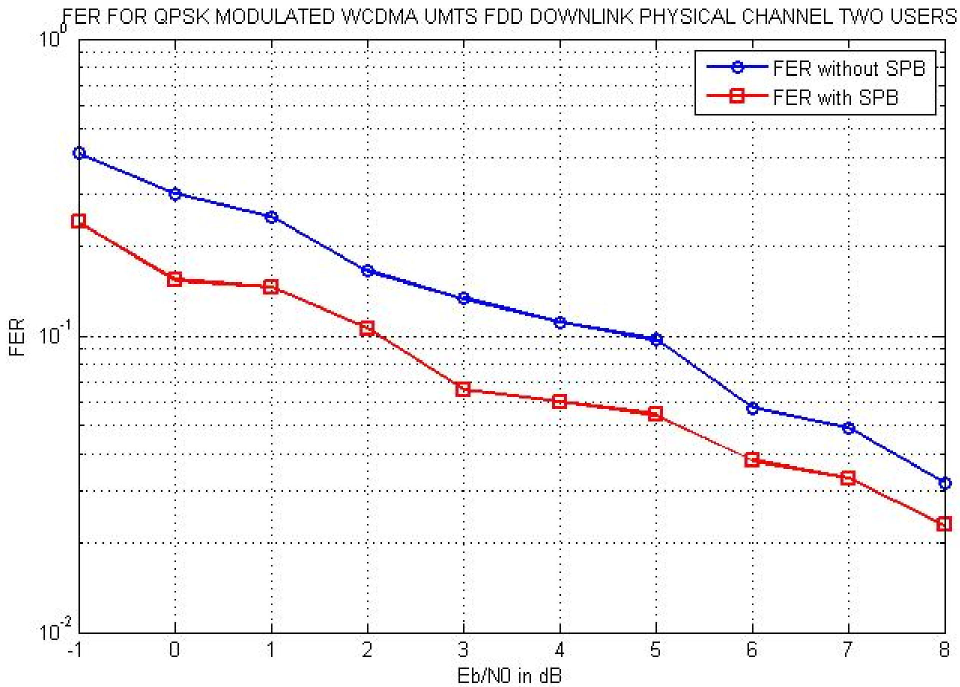

Figure 9.8 Frame error rate (FER) for QPSK modulated signal in WCDMA based UMTS FDD downlink physical channel with two users.

9.2.3.4 Frame error rate (FER) for QPSK modulated signal in WCDMA based UMTS FDD downlink physical channel with four users

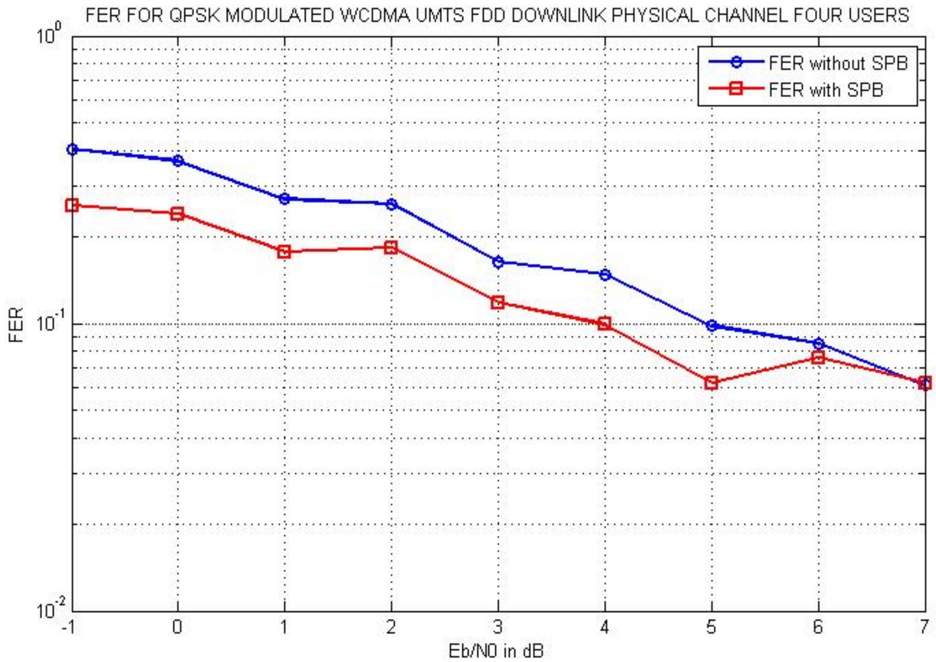

Figure 9.9 Frame error rate (FER) for QPSK modulated signal in WCDMA based UMTS FDD downlink physical channel with four users.

9.2.4 Simulation of HSDPA 3G wireless communication system

HSDPA aims to improve both the system capacity as a whole, and the data rate that can be allocated for one user as compared to UMTS systems. The maximum theoretical data rate for one user is 14.4 Mbit/s, but in real systems, this is likely to be limited to around 2 Mbit/s. The HSDPA uses HS-PDSCH (High Speed-Physical Downlink Shared channel) to provide the fast data rates [23]. (The details of HS-PDSCH are given in section 8.1.1. The block diagram of the transport layer and the physical layer operations on a HS-PDSCH frame for a single user is shown in figure 8.1.) The control information is carried through a separate channel known as the High Speed Shared Control Channel (HS-SCH).

The downlink physical layer and the transport layer operations on the data frame in HS-PDSCH for a single user are simulated in Matlab. The raw BER and FER calculations are carried out for a thousand different frames under varying channel and noise parameters for different values of SNR. The results of the simulation are plotted in figure 9.10 and 9.11 respectively. From the results, it can be concluded that the insertion of the SPB in the receiver of the system improves the performance of the system by reduction of BER and FER at low values of SNR. At higher values of SNR, the values of the BER curves with and without the SPB converge.

9.2.4.1 BER for QPSK modulated signal in HSDPA FDD downlink physical channel with single user

Characteristics	Parameters
Users	1
Channel Type	'Rayleigh'
Input Sample Period	2.6042e-007
Doppler Spectrum	Jake's Model
Maximum Doppler Shift	100 Hz
No. of Multipath	4
Path Delays	1.0e-006 * [0 0.2604 0.5208 0.7813]
Avg. Path Gains (dB)	[0 -3 -6 -9]

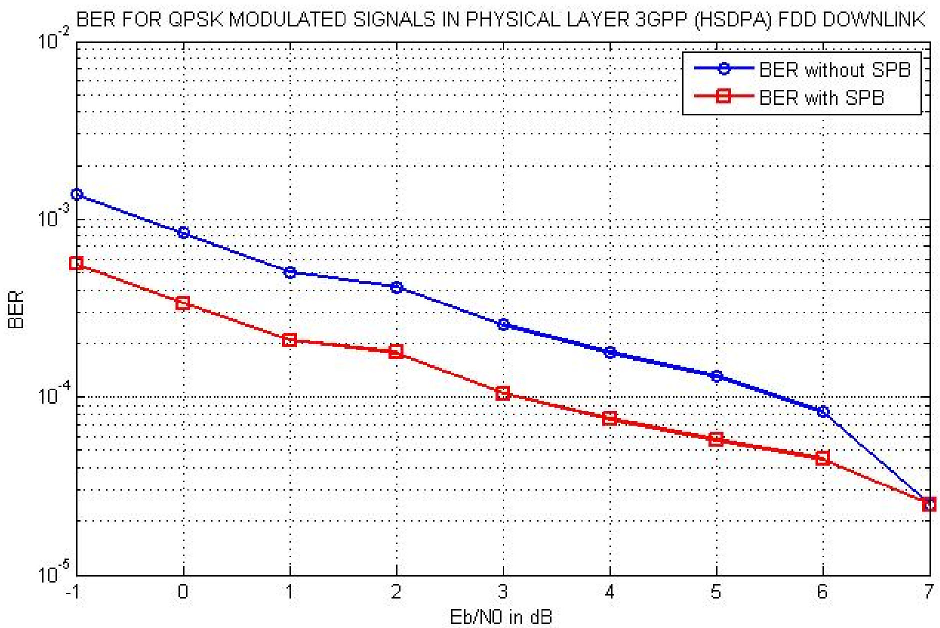

Figure 9.10 BER for QPSK modulated signal in HSDPA FDD downlink physical channel with single user.

9.2.4.2 FER for QPSK modulated signal in HSDPA FDD downlink physical channel with single user

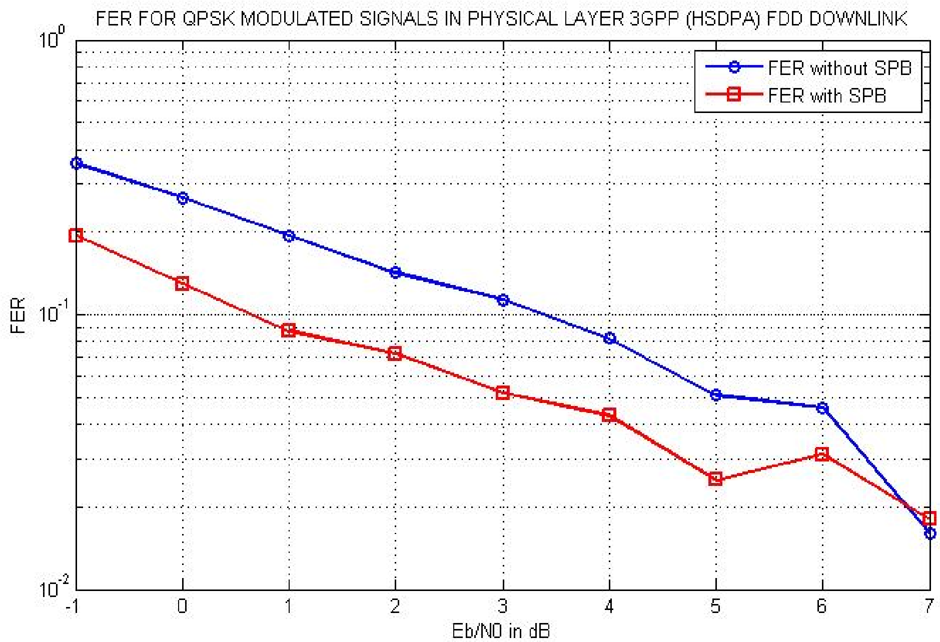

Figure 9.11 FER for QPSK modulated signal in HSDPA FDD downlink physical channel with single user.

CHAPTER 10

CONCLUSION AND FUTURE WORK

10.1 Conclusion

In this thesis, we tested the performance of our proposed signal processing block for a third generation system simulated in Matlab. Based on the simulation results, we can conclude that the addition of the SPB at the receiver reduces the BER and the FER in the system. Hence, the SPB can be used for

- Reducing call drops
- Increasing data rates and providing shorter delay in packet data communication
- Helping in the successful handover of the UE from one cell to another
- Potentially increasing the overall coverage area of the cell.

10.2 Future Work

- Implement 64QAM modulation schemes with transmit and receive diversity of higher order for a HSPA+ system and test it with SPB.
- Extend the SPB approach for 4G Long Term Evolution (LTE) cellular system with Orthogonal Frequency Division Multiple Access (OFDMA) for downlink transmission.
- Real-time implementation of the SPB.

REFERENCES

[1] S. Sharma., On reducing call drop outs by improving bit error rate performance in a GSM mobile communications system, pp. 70.

[2] K. Singh., Improving the bit error rate performance of a GSM system using an independent component analysis based non-linear filter, pp. 71.

[3] J. C. Stone, *Independent Component Analysis: A Tutorial Introduction* Cambridge, Mass.; MIT Press, 2004.

[4] Noll Michael A., "Pitch Determination of Human Speech by The Harmonic Product Spectrum, The Harmonic Sum Spectrum, and a Maximum Likelihood Estimate," *Proceedings of the Symposium on Computer Processing Communications,* pp. 779-797, 1969.

[5] A. Richardson, *WCDMA Design Handbook* New York: Cambridge Univeristy Press, 2005.

[6] H. Holma and A. Toskala, *WCDMA for UMTS: HSPA Evolution and LTE* Chichester, England; Wiley, 2007.

[7] B. Walke and M. P. Althoff, *UMTS the Fundamentals* Chichester, West Sussex, England; Wiley, 2003.

[8] T. S. Rappaport., *Wireless Communications: Principles and Practice*.

[9] M. Schwartz, *Mobile Wireless Communications* Cambridge ; Cambridge University Press, 2005.

[10] B. Sklar., Rayleigh fading channels in mobile digital communication systems .I. characterization *IEEE Communications Magazine 35(7),* pp. 90 <last_page> 100.

[11] G. L. Stüber and G. L. St ber, *Principles of Mobile Communication* Boston: Kluwer Academic, 2001.

[12] A. Hyvärinen., Independent component analysis: Algorithms and applications *Neural Networks 13(4-5),* pp. 411 <last_page> 430.

[13] 3GPP Technical Specification 25.212 "Multiplexing and channel coding (FDD) (Release 10)", www.3gpp.org

[14] 3GPP Technical Specification 25.213 "Spreading and Modulation (FDD) (Release 10)", www.3gpp.org.

[15] 3GPP Technical Specification 25.104 "Base Station (BS) radio transmission and reception (FDD) (Release 10)", www.3gpp.org.

[16] 3GPP Technical Specification 25.104 "User Equipment (UE) radio transmission and reception (FDD) (Release 10)", www.3gpp.org.

[17] 3GPP Technical Specification 25.104 "Base Station (BS) radio transmission and reception (FDD) (Release 10)", www.3gpp.org.

[18] 3GPP Technical Specification 25.214 "Physical layer procedures (FDD) (Release 10)", www.3gpp.org.

[18] 3GPP Technical Specification 25.144 "User Equipment (UE) and Mobile Station (MS) over the air performance requirements (Release 10)", www.3gpp.org.

[19] 3GPP Technical Specification 25.950 " UTRA High Speed Downlink Packet Access (Release 4)", www.3gpp.org.

[20] 3GPP Technical Specification 25.950 " High Speed Downlink Packet Access: Physical Layer Aspects (Release 5)", www.3gpp.org.

[21] 3GPP Technical Specification 25.858 " High Speed Downlink Packet Access: Physical Layer Aspects (Release 5)", www.3gpp.org.

[22] 3GPP Technical Specification 25.308 "High Speed Downlink Packet Access (HSDPA); Overall description; Stage 2 (Release 10)", www.3gpp.org.

[23] J. Korhonen, “HSDPA – An introduction”, TTPCom White Paper, www.ttpcom.com.

BIOGRAPHICAL INFORMATION

Winston Dsouza completed his Masters in Electrical Engineering in August, 2011. During his masters, he worked as RF/Electrical Engineering Co-Op at Motorola Solutions. He holds a Bachelor of Science degree in Electronics and Telecommunications from the University of Mumbai. His prime interests are in the field of broadband wireless technology and computer networks.